

**BOLU ABANT IZZET BAYSAL UNIVERSITY
THE GRADUATE SCHOOL OF NATURAL AND APPLIED
SCIENCES**



**FABRICATION OF PIN PHOTODIODE SENSORS AND
CHARACTERIZATION**

MASTER OF SCIENCE

EMRE DOĞANCI

BOLU, DECEMBER 2018

BOLU ABANT IZZET BAYSAL UNIVERSITY
THE GRADUATE SCHOOL OF NATURAL AND APPLIED
SCIENCES
DEPARTMENT OF PHYSICS



FABRICATION OF PIN PHOTODIODE SENSORS AND
CHARACTERIZATION

MASTER OF SCIENCE

EMRE DOĞANCI

BOLU, DECEMBER 2018

APPROVAL OF THE THESIS

FABRICATION OF PIN PHOTODIODE SENSORS AND CHARACTERIZATION submitted by **EMRE DOGANCI** in partial fulfillment of the requirements for the degree of **Master of Science** in **Department of Physics, The Graduate School of Natural and Applied Sciences of BOLU ABANT IZZET BAYSAL UNIVERSITY** in 26/12/2018 by

Examining Committee Members

Signature

Supervisor
Prof. Dr. Ercan YILMAZ
Bolu Abant İzzet Baysal University



.....

Member
Assoc. Prof. Dr. Ayşegül KAHRAMAN
Bursa Uludağ University



.....

Member
Asist. Dr. Oktay AYTAR
Bolu Abant İzzet Baysal University



.....

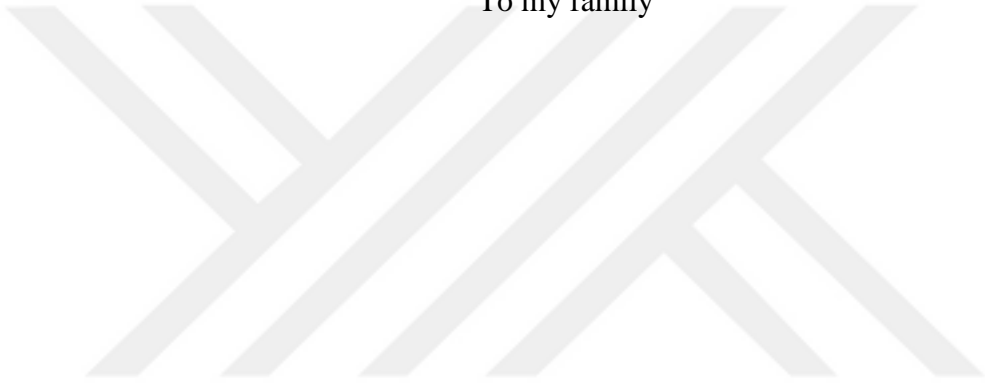
Graduation Date

: 26/ 12 / 2018

Prof. Dr. Ömer ÖZYURT

Director of Graduate School of Natural and Applied Sciences

To my family



DECLARATION

I hereby declare that all information in this document has been obtained and presented in accordance with academic rules and ethical conduct. I also declare that, as required by these rules and conduct, I have fully cited and referenced all material and results that are not original to this work.

EMRE DOĞANCI

ABSTRACT

FABRICATION OF PIN PHOTODIODE SENSORS AND CHARACTERIZATION MSC THESIS

EMRE DOĞANCI

BOLU ABANT IZZET BAYSAL UNIVERSITY GRADUATE SCHOOL OF
NATURAL AND APPLIED SCIENCES

DEPARTMENT OF PHYSICS
(SUPERVISOR: PROF. DR. ERCAN YILMAZ)

BOLU, DECEMBER 2018

p-type, intrinsic, n-type (PIN) photodiodes with active areas of $3.5 \times 3.5 \text{ mm}^2$, $5.0 \times 5.0 \text{ mm}^2$, and $7.0 \times 7.0 \text{ mm}^2$ were fabricated using the conventional photolithography method on a 6 inch (100) intrinsic silicon wafer with a surface resistivity of $2.4 \text{ k}\Omega - 2.8 \text{ k}\Omega$ at $500 \text{ }\mu\text{m}$ thicknesses. n and p regions were formed using the phosphorus (POCl_3) and boron (BBr_3) doping at $950 \text{ }^\circ\text{C}$ via thermal diffusion method. As expected for the capacitance-voltage (C-V) characteristic of the fabricated PIN photodiodes decreases exponentially with the reverse-biased voltage. The capacitance of each PIN diode reached a fully depleted point at -5V . The capacitance was measured at the fully depleted point as the order of pF. The dark current-voltage (I_d -V) characteristics of the PIN diodes were measured at room temperature in the reverse biased. Thanks to the structure of the PIN diodes, they have worked on high voltages without breakdown. However, due to the effects of high voltage and the effects of silicon temperature dependency, the dark current is observed in μA at breakdown voltage. At lower voltages, the dark currents drop to nA. Silicon PIN photodiodes, which are produced according to the results of quantum efficiency and spectral responses, can detect wavelengths between 380 nm and 1100 nm and have reached maximum efficiency at 810 nm wavelength. The fabricated PIN diodes can be used in optoelectronic applications.

KEYWORDS: Silicon PIN Diode, Photodiode Fabrication, Quantum Efficiency, Dark Current, Capacitance

ÖZET

PIN FOTO DİYOT SENSÖRLERİNİN ÜRETİMİ VE KARAKTERİZASYONU YÜKSEK LİSANS TEZİ

**EMRE DOĞANCI
BOLU ABANT İZZET BAYSAL ÜNİVERSİTESİ
FEN BİLİMLERİ ENSTİTÜSÜ**

**FİZİK ANABİLİM DALI
(TEZ DANIŞMANI: PROF. DR. ERCAN YILMAZ)**

BOLU, ARALIK - 2018

3.5x3.5 mm², 5.0x5.0 mm² ve 7.0x7.0 mm² aktif alana sahip p-bölge, saf, n-bölge (PIN) foto diyotlar 500 µm kalınlığında 2.4 kΩ - 2.8 kΩ yüzey direncine sahip (100) yönelimli saf silikon alt taş üzerine geleneksel fotolitografi metodu kullanılarak üretilmiştir. Üretim sırasında farklı taşıyıcı yüklere sahip n ve p bölgeleri fosfor (POCl₃) ve boron (BBr₃) katkılanması termal difüzyon yöntemi kullanılarak 950 °C oluşturulmuştur. Üretilen PIN foto diyotların kapasitans voltaj (C-V) karakteristiği beklendiği gibi her bir PIN diyotun kapasitans değerlerinde uygulanan ters kutuplama voltajı ile üstel bir şekilde azalma gözlenmiştir ve diyotlar -5V voltta doyum noktasına ulaşmıştır. Doyum noktasındaki kapasitans değerleri pF mertebesinde ölçülmüştür. PIN diyotların karanlık akım (I_d-V) değerleri ters kutuplama oda sıcaklığında ölçülmüştür. PIN foto diyotlar sahip olduğu yapı sayesinde yüksek voltajlarda bozulma olmadan çalışmaktadır. Fakat yüksek voltajın etkisi ve silikonun sıcaklıktan etkilenmesi nedeniyle oluşan karanlık akım değerleri µA mertebesinde gözlenmiştir. Daha düşük voltajlarda ise karanlık akım değerleri nA mertebelerine kadar düşmüştür. Kuantum verimliliği ve spektral cevap sonuçlarına göre üretilen Silikon PIN foto diyotlar 380 nm-1100 nm arasındaki dalga boylarını algılayabilmektedir ve 810 nm dalga boyunda maksimum verimliliğe ulaşmaktadır. Üretilen PIN diyotlar optoelektronik uygulamalarda kullanılabilir.

ANAHTAR KELİMELER: Silikon PIN Diyot, Fotodiyot üretimi, Kuantum Verimliliği, Karanlık akım, Kapasitans

TABLE OF CONTENTS

	<u>Page</u>
ABSTRACT	v
ÖZET	vi
TABLE OF CONTENTS	vii
LIST OF FIGURES	ix
LIST OF TABLES	xi
LIST OF ABBREVIATIONS AND SYMBOLS	xii
1. INTRODUCTION	1
2. AIM AND SCOPE OF STUDY	3
3. GENERAL SEMICONDUCTOR PHYSICS	4
3.1 General Characteristics of Semiconductors	5
3.1.1 Intrinsic Semiconductors	6
3.1.2 Extrinsic Materials	6
3.2 Theory of carrier transport and P-N junction operation	8
3.2.1 Photovoltaic Mode	10
3.2.2 Photoconductive Mode	10
3.3 Overview of Silicon PIN photodiode	11
3.3.1 Theory of Silicon PIN Photodiode.....	11
3.3.2 The Advantage of Silicon PIN Photodiode.....	12
3.4 Electrical Characteristic Silicon PIN Photodiode.....	13
3.4.1 Current-Voltage Characteristic	13
3.4.2 Capacitance-Voltage Characteristic.....	14
3.4.3 Quantum Efficiency and Spectral Response.....	15
4. MATERIAL AND METHODS	18
4.1 Fabrication of Silicon PIN Photodiode	18
4.1.1 Cleaning Process of Silicon Wafer	18
4.1.2 Initial Field Oxide Deposition	19
4.1.3 Photolithography Process for Phosphorus Deposition.....	20
4.1.4 Photolithography Process for Boron Deposition	22
4.1.5 Photolithography Process for Metallization	23
4.2 Device Characteristic of Silicon PIN Photo Diode	26
4.2.1 Current-Voltage Characteristic Measurement	26
4.2.2 Capacitance-Voltage Characteristic Measurement.....	27
4.2.3 Quantum Efficiency and Spectral Response Measurement.....	28
5. EXPERIMENTAL RESULTS AND DISCUSSIONS	29
5.1 Measurement Results of Fabricated Silicon PIN Photodiode	29
5.1.1 Results of Capacitance -Voltage Characteristic.....	29
5.1.2 Results of Current-Voltage Characteristic	31
5.1.3 Results of Quantum Efficiency and Spectral Response.....	33
6. CONCLUSION AND RECOMMENDATION	35

7. REFERENCES37
8. CURRICULUM VITAE41



LIST OF FIGURES

	<u>Page</u>
Figure 3.1. Band structure of materials a) Insulator b) Semiconductor c) Conductor	4
Figure 3. 2. Energy band gap changing with absolute temperature	5
Figure 3. 3. Chemical representation of boron bonding with silicon	7
Figure 3. 4. Acceptor energy level after boron deposition.....	7
Figure 3.5. Chemical representation of phosphorus bonding with silicon	8
Figure 3.6. New energy level structure after phosphorus deposition.....	8
Figure 3.7. Representation of P-N Junction and its band diagram.....	9
Figure 3.8. Photovoltaic mode operation representation.....	10
Figure 3.9. Photoconductive mode operation representation	11
Figure 3.10. Silicon PIN photodiode structure and band diagrams	12
Figure 3.11. General current-voltage characteristic of silicon PIN photodiode	14
Figure 3.12. a) Ideal responsivity characteristic b) Quantum efficiency of materials	17
Figure 4.1. Spectroscopy measurement of a silicon wafer.....	19
Figure 4.2. Silicon Oxide on a silicon wafer.....	19
Figure 4.3. The photoresist on a silicon wafer	20
Figure 4.4. Ultraviolet exposure on a silicon wafer	20
Figure 4.5. Silicon wafer representation after initial lithography	21
Figure 4.6. a) Wafer structure after phosphorus deposition process b)Wafer structure after drive-in the process	21
Figure 4.7. Photolithography process for boron deposition	22
Figure 4.8. a) Wafer structure after boron deposition b) Wafer structure after drive-in the process	23
Figure 4. 9. Ultraviolet light exposure	23
Figure 4.10. Wafer structure after liftoff process.....	24
Figure 4.11. Ultraviolet exposure on a silicon wafer to spoil photoresist.....	24
Figure 4.12. Schematic representations of PIN photodiode structure.....	25
Figure 4.13. Fabricated PIN photodiode structure	25
Figure 4.14. I-V measurement system	26
Figure 4.15. C-V measurement system	27
Figure 4.16. Spectral responsivity and quantum efficiency measurement system..	28
Figure 5.1. a) Reverse biased C-V and C^{-2} -V characteristics $3.5 \times 3.5 \text{ mm}^2$ PIN diode b) Reverse biased C-V and C^{-2} -V characteristics $5.0 \times 5.0 \text{ mm}^2$ PIN diode c) Reverse biased C-V and C^{-2} -V characteristics $7.0 \times 7.0 \text{ mm}^2$ PIN diode	30
Figure 5.2. a) Reverse biased dark current measurement at 295K b) Reverse dark current density function of the PIN photodiode active area at -5V	32

Figure 5.3. a) Quantum efficiency measurement characteristic b) Spectral responsivity measurement characteristic.....33



LIST OF TABLES

	<u>Page</u>
Table 1. Some electrical parameters of fabricated PIN photodiodes	31
Table 2. Quantum efficiency and Spectral response results.....	34



LIST OF ABBREVIATIONS AND SYMBOLS

A	: Junction Area
c	: Speed of Light
C-V	: Capacitance - Voltage Characteristic
E_g	: Band Gap Energy
f(E)	: Fermi Energy
f	: Frequency
g_{ph}	: Generated Electron-Hole
h	: Planck Constant
I-V	: Current-Voltage Characteristic
I_L	: Load Current
I_p	: Photo Current
I_{sat}	: Saturation Current
I_d	: Dark Current
k_b	: Boltzmann Constant
k_o	: Dielectric Constant
L_n	: Diffusion Length of N-type
L_p	: Diffusion Length of P-type
N_D	: Impurity concentration of Donor Region
N_p	: Impurity concentration of Acceptor Region
n_i	: Impurity concentration of Intrinsic Region
P₀	: Optical Power
R	: Responsivity
R_f	: Feedback Resistor
r_e	: Electron Number
r_p	: Incident Photon
RCA	: Radio Corporation of America
T(K)	: Temperature in Kelvin
V_A	: Applied Voltage
V_r	: Reverse Voltage
V_{out}	: Output Voltage
q	: Electron charge
W	: Depletion Region Wide

λ_p : Peak Wavelength
 λ : Wavelength
 η : Quantum Efficiency
 η_{in} : Internal Quantum Efficiency
 ϵ : Material Permittivity



ACKNOWLEDGEMENTS

I wish to express my deepest gratitude to my supervisor, Prof. Dr. Ercan YILMAZ for his guidance, advice, criticism, and support throughout this thesis and also with my professional development.

I would like to thank Assoc. Prof. Dr. Aliekber AKTAĞ for his suggestions and comments. I would also like to express my deep appreciation to my colleagues, and they are also my teachers, Dr. Şenol KAYA and Ramazan LÖK for their help, sincerity, hospitality, and friendship.

I offer special thanks to Prof. Dr. Raşit TURAN and his student Elif SARIGÜL for helping with the measurement.

Finally, I am very grateful to my amazing parents: Dad, Adnan DOĞANCI, Mom, Hayriye DOĞANCI, Sister, Elif GÖKÇE, her husband Mutlu GÖKÇE for their love, moral support, constant encouragement, and prayers throughout this process.

This thesis was supported in part by the Ministry of Development, Turkey, under Contract No: 2012K120360 and 2016K121110, and in part by Bolu Abant İzzet Baysal University, Bolu, Turkey, BAP Project under Contract No: 2017.03.02.1153

1. INTRODUCTION

P-N junction structure has a vital role in the development of semiconductor devices such as thyristors, a bipolar transistor, solar cell, tunnel diode, and photodiode etc. (Sze, 2002). In the twentieth century, P-N junction diode that was fabricated for detection light to convert into electric current is called a photodiode. In order to fabricate this photodiode, optical photolithography process was used to pattern wafers. For this purpose, wafers are covered with photoresist and then these wafers are illuminated with a light beam to remove photoresist. This process was subsequently used to define the region by using silicon dioxide masking with which boron and phosphorus diffusion are effectively masked while creating a P-N junction. The P-N photodiode was found more useful than gas-ion chamber as a radiation detector (Barthe, 2001; Kemmer, 1984). However, Simple P-N junction photodiode suffers from some problems such as narrow depletion region, high capacitance, low breakdown voltage, which are so crucial for a photodetector because high capacitance directly affects the speed of photodiode. Capacitance can be reduced with widened depletion region but break down phenomena is occurred at low voltage because of semiconductor characteristic structure. Therefore high reverse biased cannot be used to wide depletion region (Ahmed, 2007; Sze, 2007).

To cope up with these issues, the new p-type, intrinsic region, n-type (PIN) structure has been utilized for photodiode detectors. High resistivity intrinsic region in photodiode creates widened depletion region without reverse voltage and reduce capacitance. In addition, the PIN photodiode reaches full depletion mode at the low reverse voltage and so the PIN photodiode possesses low operation power to work (Kyomasu, 1995). So, PIN photodiodes have been fabricated with different geometric arrangements by using different semiconductor materials such as Silicon (Si), Indium Gallium Arsenide (InGaAs), Germanium (Ge) for decades. These used materials affect directly PIN photo diode's operational and optical behavior. III-V materials, Gallium Arsenide, and Indium Gallium Arsenide are generally preferred for longwave electronics application such as communication and radar system. However, among these materials, Silicon is most convenient semiconductor for

radiation detector due to its low cost, band structure, long carrier lifetime and wide detection range. Also, high- quality silicon dioxide layer can be easily grown onto silicon (Ben and Sanjay, 2005; Bowers and Burrus, 1987; Kemmer, 1984; Luryi et al., 1984; Nicollian and Brews, 2003; Tucker et al., 1986; Von Ammon and Herzer, 1984; Wood and Burrus, 1984; Yamamoto et al., 1987).

Most of the researches focus on the mechanism and the reduction of leakage current which causes non-linearity on the PIN photodiode and it was reduced significantly with planar structure and silicon dioxide passivation (Feng et al., 2018; Resnik et al., 2000). Floating guard ring was also found effective on reducing leakage current (Mishra et al., 2005). In addition, fabrication methods such as thermal deposition, ion implantation, and different dopant concentrations were also utilized for PIN photodiodes performance improvements and capacitance was reduced to the rank of pico-farad. Thus, the high detection response speed was obtained (Yamamoto et al., 1995; Zhou and Warburton, 1996). Another important parameter for PIN photodiode is quantum efficiency on which many factors effective like dopant thickness of p type, intrinsic region and n type, and band gap. In light of this information, the spectral range of Silicon PIN photodiodes was found between 190 nm and 1100 nm and maximum quantum efficiency is obtained near-infrared region (Goushcha et al., 2004; Sze, 1985).

After these developments as to PIN photodiode, crucial results have been obtained in the field of energy physics, a radiation sensor, personal dosimeter, diagnostic radiology, and digital image application. This situation makes PIN photodiodes more attractive commercially (Kim et al., 2014; Seto et al., 1997; Simon and Kalinka, 2005).

Concisely, purpose of the Silicon PIN photodiode is that when radiation hits the active area of the photodiode, electron and hole pairs are created inside the depletion region (depleted intrinsic region). These carries move opposite direction by the way of the electric field of the depletion region and constitute an electrical current. This current can be changeable according to environmental condition and structural differences (Kumar et al., 2014). So, parameters influences on the PIN photodiode device characteristics have been investigated in details in this thesis.

2. AIM AND SCOPE OF STUDY

The aim of this thesis study is to fabricate and characterize planar silicon PIN photodiodes which have different active areas. During the fabrication process, the photolithography and wet-chemical etching were carried out to define doped areas. The N⁻ doped regions were formed by phosphorus diffusion (using POCl₃), and P⁺ regions by boron diffusion (using BBr₃). PIN photodiodes have been characterized electrically and optically. In order to do this application, Current-Voltage (I-V) characteristic and Capacitance-Voltage (C-V) characteristic have been carried out on photoconductive mode under dark condition. In addition, quantum efficiencies of silicon PIN photodiodes have also been measured under the light that has a different wavelength to determine maximum efficiency.

3. GENERAL SEMICONDUCTOR PHYSICS

Solid state materials are classified into three types as an insulator, semiconductors, conductor which contain different band structure shown Figure 3.1.

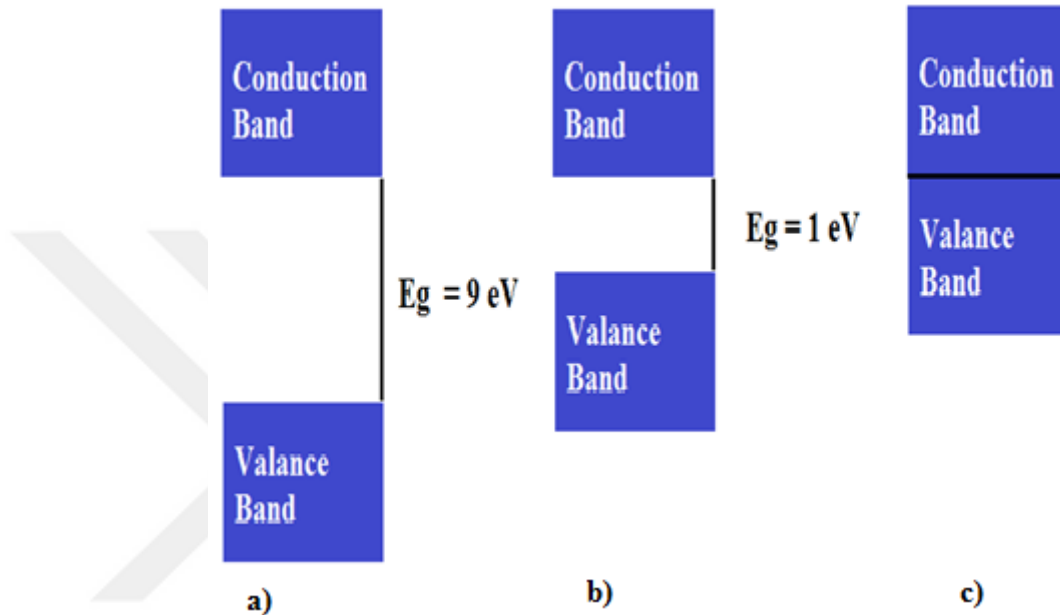


Figure 3.1. Band structure of materials a) Insulator b) Semiconductor c) Conductor

Insulator materials' atoms have strong covalent bonds with neighbouring atoms, so too much energy is necessary to break these bonds. This situation results in an electrical current absence. Insulator materials' characteristic band structure is defined with large energy band which is about 9 eV and all energy levels are occupied by electrons in the valence band. Conduction band is vacant because thermal energy or applied electric field cannot supply adequate energy for electrons to jump from valence band to conduction band. Semiconductors have an energy band whose energy in there about 1eV and all electrons are in the valence band and conduction band is empty at absolute zero. So, semiconductor materials are a wimpy conductor at low temperature. Metal has so low resistivity and there is no energy band. Because of this, electron can gain kinetic energy to move with small electric field and thermal excitation. Solid state materials show different electrical features that are changeable according to their electrical conductivity, and resistivity. But

semiconductor materials additionally have sensitivity to magnetic field, temperature, and illumination. Therefore, semiconductors most commonly used for technological devices fabrication (Sze, 2002).

Overs years, many studies have been studied and investigated the conductivity and resistivity of semiconductors that is between $10^{-2} \Omega\text{cm}$ and $10^9 \Omega\text{cm}$, 10^1 S/cm and 10^{-8} S/cm (Kittel, 2005; Sze, 2002).

3.1 General Characteristics of Semiconductors

Silicon is the most preferred semiconductor with its low cost and purified form. This purified form possesses intrinsic concentration and resistivity, which makes silicon available for electronic device fabrication. Another important characteristic structure of the silicon is its bandgap which is not as low as germanium and is not as high as Gallium Arsenide. This band structure of silicon enables impurity adding process to reach desired properties. Temperature effects on silicon band structure such as another semiconductor are shown in Eq 1.

$$E_g = 1.17 - 4.73 \times 10^{-4} \frac{T^2}{T+636} \quad (1)$$

E_g is band gap energy in eV and T is the absolute temperature. According to this formula, Silicon characteristic is plotted in Figure 3.2.

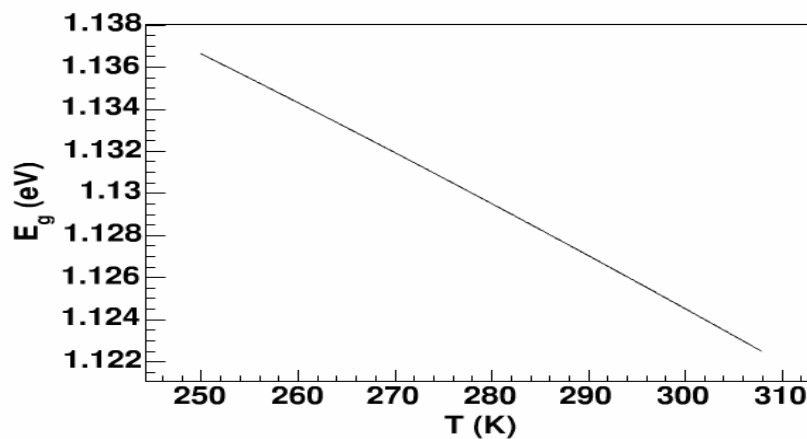


Figure 3. 2. Energy band gap changing with absolute temperature (Ahmed, 2007)

Temperature differences cause band gap changes, like widening and shortening. These differences are not good because small band gap enables to generated electron-hole pair to pass from valence band to conduction band under the same irradiation. This situation can cause nonlinearity on integrated circuit component (Ahmed, 2007).

3.1.1 Intrinsic Semiconductors

Intrinsic semiconductor materials are called as un-doped materials due to the fact that the intrinsic material has a little number of free charges that are produced the bulk of semiconductor crystals. These charges occupy different energy state and this separation is explained by Boltzmann distribution as shown in Eq 2.

$$f(E) = \frac{1}{1 + e^{(E-E_F)/k_B T}} \quad (2)$$

Where E is the energy of the electron, k_B is Boltzmann constant, T is absolute temperature. $f(E)$ is the Fermi function.

Available energy state for electron occupancy probability is calculated with Fermi function. In intrinsic semiconductors, the Fermi level is located in the middle of the energy band, so the amount of electron and holes are in equilibrium in intrinsic semiconductor materials as well as their probability is $\frac{1}{2}$ because Electron energy is equal to Fermi energy. (Ahmed, 2007; Boylestad, 2013)

3.1.2 Extrinsic Materials

Extrinsic materials consist of impurities that are doped. Deposition application results in significant changes and improves the performance on semiconductor materials. Extrinsic materials are created by doping process that is adding small impurities to intrinsic materials. These impurities have a different number of electrons in its outer atomic shell. This situation composes a new energy level between conduction and valence band.

This energy levels position depends on used impurities that are donor and acceptor. Donor impurities make semiconductors more negative. Acceptor impurities

make abundant semiconductor in positive charge. Boron and phosphorus are most commonly used materials to create p-type and n-type (Boylestad, 2013).

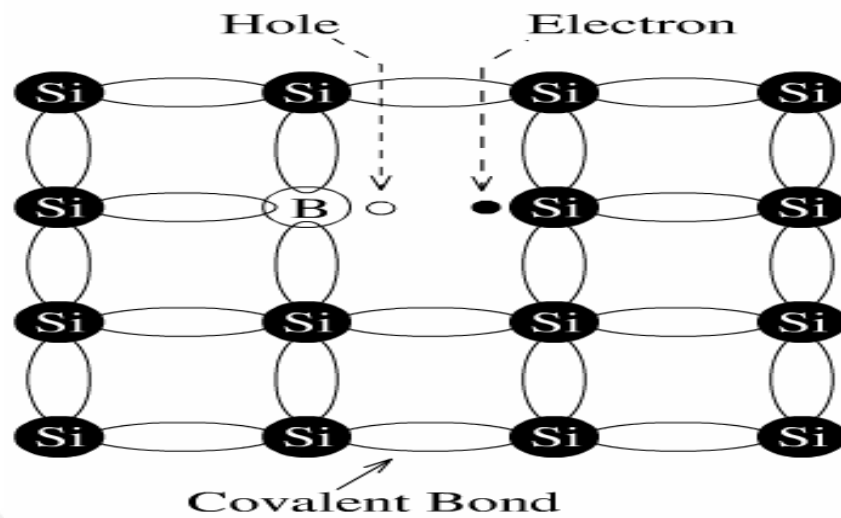


Figure 3. 3. Chemical representation of boron bonding with silicon (Ahmed, 2007)

In Figure 3.3. Silicon makes covalent bonding with its neighbouring atom when boron doped in silicon structure, and doped silicon becomes more positive material. For, boron has three free electrons in the outer shell. These electrons make three bonding with Silicon atoms and leave one hole. Also new energy level is more close to valance band (Figure 3.4) due to this silicon turns into p type materials.

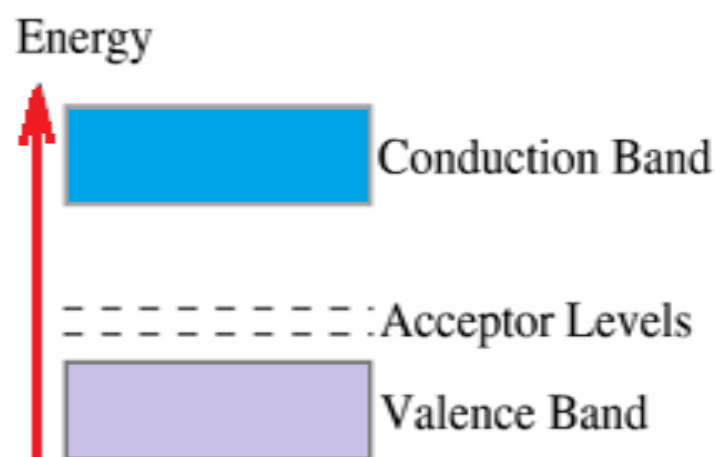


Figure 3. 4. Acceptor energy level after boron deposition

Phosphorus is doped in intrinsic Silicon turns into more abundant in negative charge. Because, Phosphorus has five electrons in the outer shell, and these electrons make bonding with Silicon atoms which leave one electron at the end (Figure 3.5).

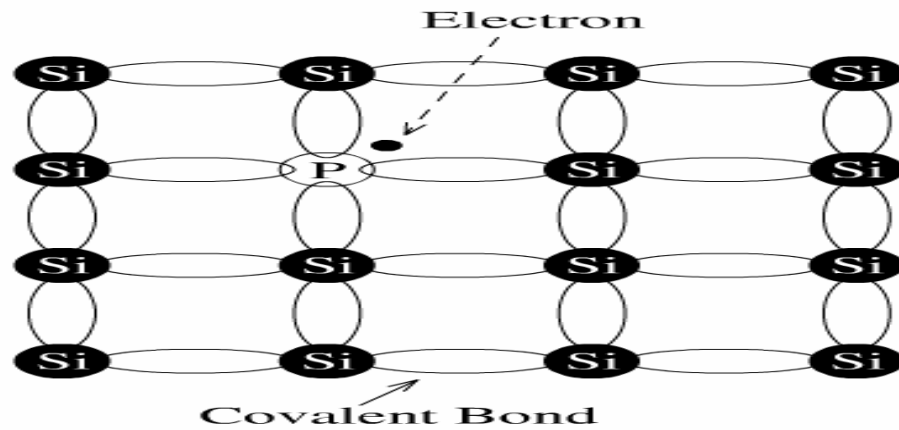


Figure 3.5. Chemical representation of phosphorus bonding with silicon (Ahmed, 2007)

In addition, Phosphorus creates a new energy level that is close to the conduction band (Figure 3.6)(Ahmed, 2007; Boylestad, 2013).

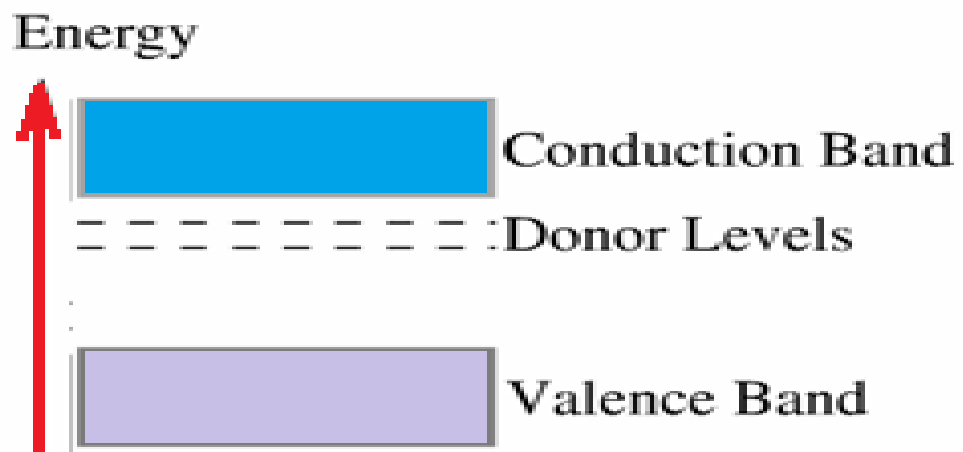


Figure 3.6. New energy level structure after phosphorus deposition

3.2 Theory of carrier transport and P-N junction operation

P-type and N-type materials come together and create the most popular PN junction. High concentration of electrons in n types and excessive hole concentration in P-type result in carrier diffusion current in which electron mobility is from N side

to P side and hole mobility is from the P side to N side. In time, progress charges are collected near the junction and deplete it. This region is called depletion region. In the basic physic principle;

Every moving particle that has charge creates an electric field. This electric field forces holes to flow from left to right, but the gradient of concentration forces holes to flow from right to left. This electric field reaches to the adequate strength which stops diffusion current and creates an equilibrium situation. PN junction structure and its band diagram are represented in Figure 3.7.

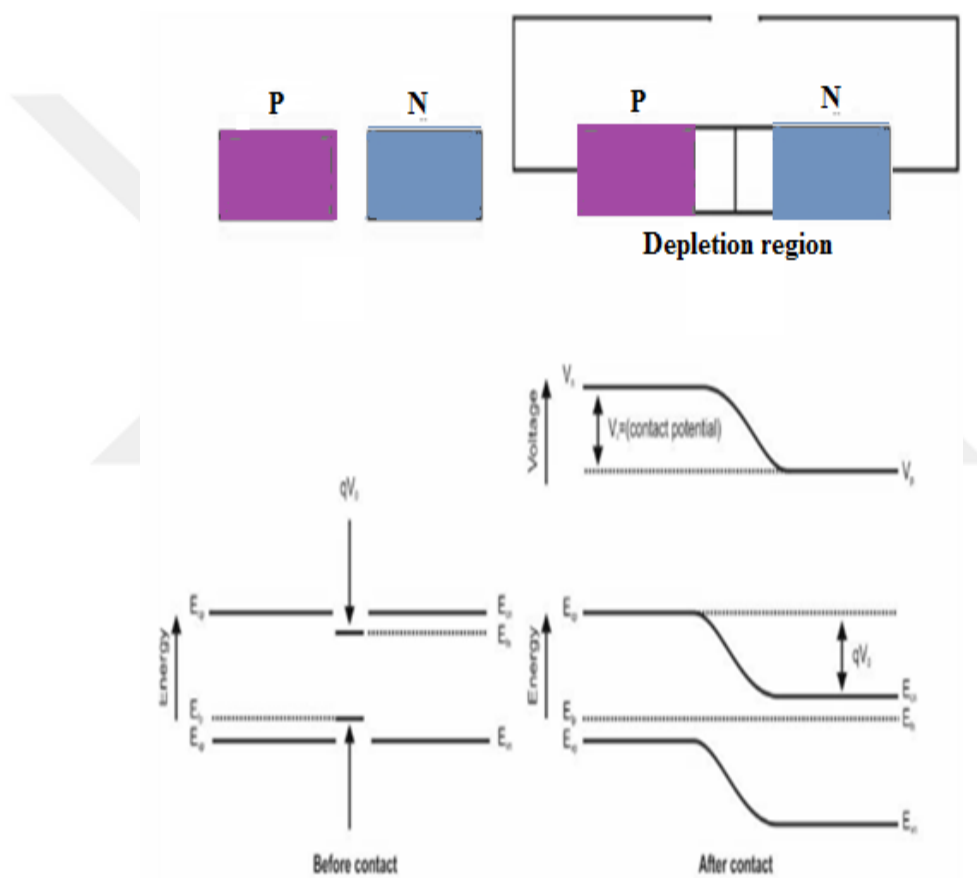


Figure 3.7. Representation of P-N Junction and its band diagram

The simple PN junction is used in the radiation detector, photovoltaic cell, and photodiode. For this purpose, depletion works as an active area in which radiation creates an electron-hole pair and result in electrical current. So PN junction can be operated in photovoltaic and conductive mode (Razavi, 2015) (Gray, 2006).

3.2.1 Photovoltaic Mode

In this mode, the large load resistance is applied to the simple P-N junction. Because of this, there is no electrical current flowing through the depletion region and the only potential difference is occurred across the diode. Electron-hole pairs are created by radiation. This current is called radiation-induced reverse current. The consequence of this flow of charges is the reduction in the junction barrier, which starts another current but now in opposite direction to I_f . This current is called as the forward current. In the photovoltaic mode in the diode is working open circuit. Therefore, the reverse current is balanced by the forward current and both of these currents are equal to each other and almost no current is appeared in circuit. This mode is generally used for solar cell application.

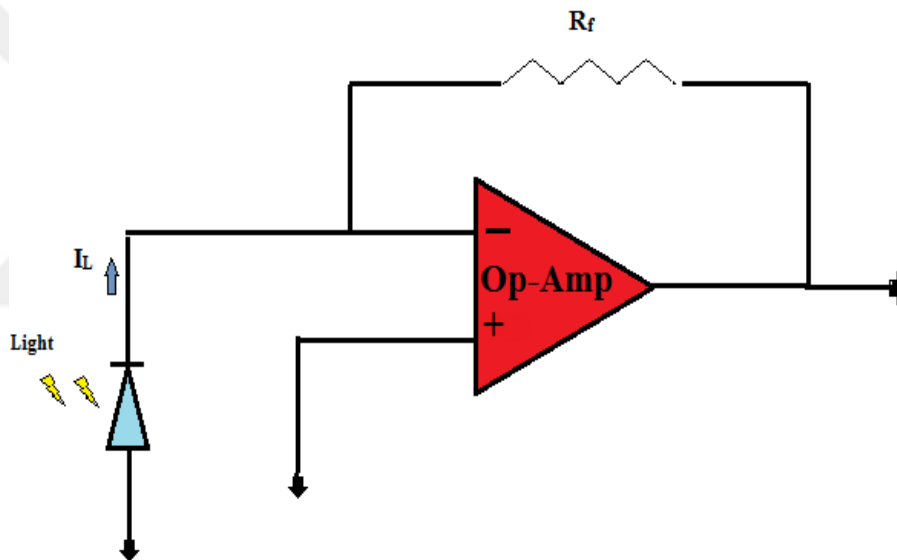


Figure 3.8. Photovoltaic mode operation representation

In Figure 3.8 P-N photodiode is working high load mode (open circuit). This means there is no reverse biased and ground connection (Ahmed, 2007).

3.2.2 Photoconductive Mode

In this mode, high reverse biased is applied across the diode and this reverse biased expands the depletion region. When radiation passes through the depletion region, an electron-hole pair is generated that constitutes electrical current under an electric field of reverse biased in Figure 3.9. The photoconductive mode is available

for the detector application because widened depletion region with reverse biased decrease capacitance of junction and increase signal noise ratio. (Ahmed, 2007)

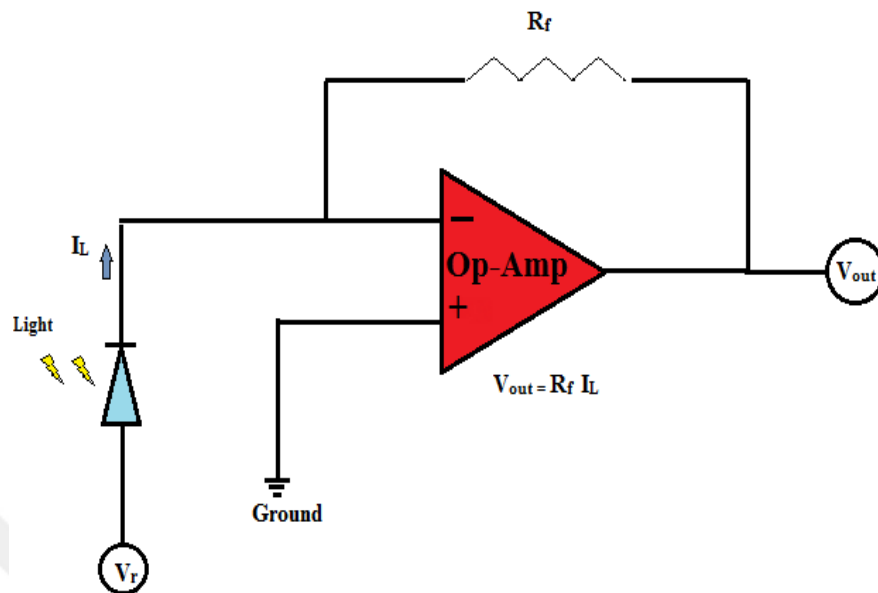


Figure 3.9. Photoconductive mode operation representation

3.3 Overview of Silicon PIN photodiode

3.3.1 Theory of Silicon PIN Photodiode

Silicon PIN photodiode basically operates similarly to PN junction. P^+ and N^- types are divided by intrinsic region. Incident radiation creates electron-hole pairs inside the PIN photodiode. The surplus electron on P^+ types and surplus holes on N^- types go through PN junction. These charges reach to the junction, and then charges pass the junction and constitute an electrical current. Silicon PIN photodiode structure is shown in Figure 3.10.

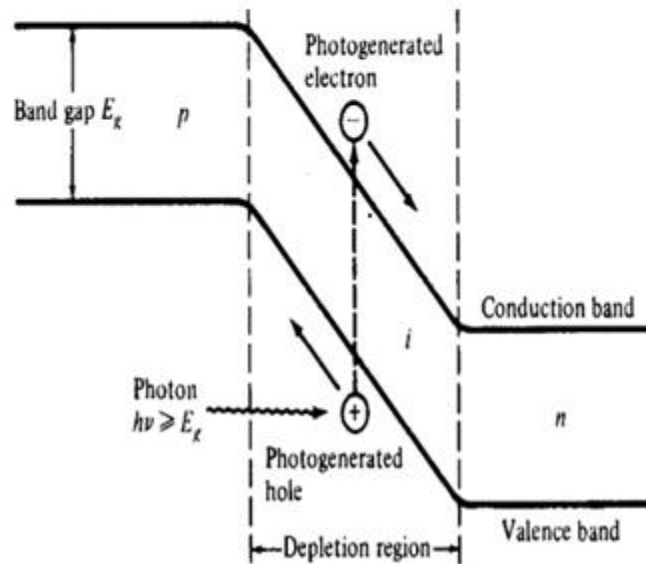


Figure 3.10. Silicon PIN photodiode structure and band diagrams

3.3.2 The Advantage of Silicon PIN Photodiode

Silicon P-N photodiode is used commonly but it suffers many problems due to its structure. In photodetector, depletion region must be wide as much as possible to deposit more radiation energy to produce electrical current. So more reverse voltage is needed to expand depletion. But Silicon crystal structure doesn't permit it to increase reverse voltage due to break down voltage. On the other hand, these issues can be solved with high resistivity intrinsic materials between P-type and N-type (Figure 3.10). Intrinsic region creates a widened depletion region without high reverse biased. These small structural differences not only expand depletion region but also decrease capacitance that arises in high-speed response. (Gray, 2006; Kumar et al., 2014)

3.4 Electrical Characteristic Silicon PIN Photodiode

3.4.1 Current-Voltage Characteristic

Current-Voltage characteristic of Silicon PIN photodiode under dark condition behaves just as the rectifying diode and operates with forward biased and reverse biased. When the photodiode is forward biased, exponential current is observed to be rising. On the other hand, if PIN photodiode is reversed biased, the leakage current is observed, which is called dark current, is shown in Eq. (3).

$$I_D = I_{SAT} \left(e^{\frac{q V_A}{K_B T}} - 1 \right) \quad (3)$$

Where I_D is dark current, I_{SAT} is saturation current, q is electron charge, V_A is applied voltage, K_B is Boltzmann constant and T is absolute temperature.

When PIN photodiode is put under light, photocurrent I_p shifts the dark current. This situation is expressed in Eq. (3.1)

$$I_D = I_{SAT} \left(e^{\frac{q V_A}{K_B T}} - 1 \right) - I_p \quad (3.1)$$

$$I_p = q g_{ph} A \left(W + L_n + L_p \right) \quad (3.2)$$

In Eq. (3.2) q is electron charge, g_{ph} refers to generated electron hole pairs per second per unit volume, A refers to an active area, W is depletion region wide, L_n and L_p diffusion length of N type and P type (Menon et al., 2004; Xu, 2015).

When PIN photodiode reaches saturation current, reverse current increases sharply because of breakdown phenomena. This situation indicates that the photodiode reaches the breakdown voltage. Characteristic of the photodiode is represented in Figure 3.11.

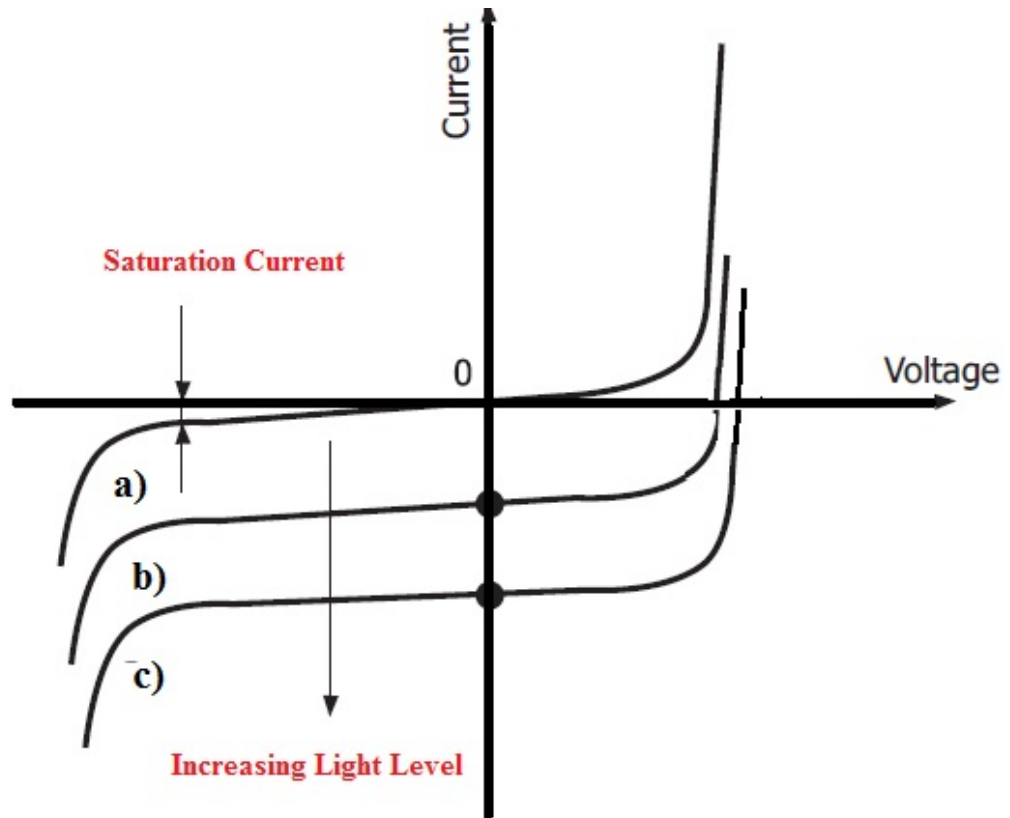


Figure 3.11. General current-voltage characteristic of silicon PIN photodiode

3.4.2 Capacitance-Voltage Characteristic

Capacitance is the most crucial parameter on photodiodes operation such as frequency response, limiting noise of the amplifier. We told about it in section 3.2.2 and in this section, we detailed what effects photodiode capacitance. A PN junction operating under reverse biased, more positive charges occur in n side and more negative charges occur in the P⁺ side so the device works as a capacitor. In other word, we can see PN junction as two plate capacitor (Razavi, 2015). This operational structure is an ability to calculate the length of the P side "L_p" and length of the N side "L_N" by using applied biased voltage V_o - V_b with following equations.

$$N_A L_P = N_D L_N \quad (4)$$

Length of N⁻ and P⁺ are varied with the concentration of impurity (N_A and N_D)

$$L_P = \left[\frac{2\epsilon N_D (V_0 - V_b)}{q N_A (N_A + N_D)} \right]^{\frac{1}{2}} \quad (4.1)$$

$$L_N = \left[\frac{2\epsilon N_A (V_0 - V_b)}{q N_D (N_A + N_D)} \right]^{\frac{1}{2}} \quad (4.2)$$

Summation of P^+ and N^- side length gives us the collective width of the depletion region.

$$W = L_P + L_N = \left[\frac{2\epsilon N_A + N_D (V_0 - V_b)}{q N_A N_D} \right]^{\frac{1}{2}} \quad (4.3)$$

Junction capacitance is written as,

$$C_j = \epsilon \frac{A}{W} = k_0 \epsilon_0 \frac{A}{W} \quad (4.4)$$

In equation k_0 is a dielectric constant of the semiconductor material, ϵ_0 is a permittivity of free space, and A is called as junction area.

We can easily notice from Eq. (4.4). Junction capacitance is inversely proportional to depletion region-wide (Ma et al., 2010; Rieke, 2002).

3.4.3 Quantum Efficiency and Spectral Response

Quantum efficiency is one of the significant optical features for the photodetector and is expressed mathematically ratio of the number of electrons collected and a number of incident photons in Eq. (5). It is determined by the absorption coefficient of semiconductor materials that are used within semiconductor materials.

$$\eta = \frac{\text{number of electrons collected}}{\text{number of incident photons}} \quad (5)$$

It can also be defined as,

$$\eta = \frac{r_e}{r_p} \quad (5.1)$$

Where r_e is electron number because of incident light, r_p is referred to incident photons on the photodetector. Internal quantum efficiency is also defined as in Eq. (5.2)

$$\eta_{in}(\lambda) = \frac{1.24 S(\lambda)}{[1-R(\lambda)]\lambda} \quad (5.2)$$

When radiation hits the photodiode which doesn't completely reach the depletion region due to surface reflections, This situation results in electron-hole recombine far away depletion region and doesn't constitute electrical current. (Goushcha et al., 2004; Gray, 2006; Onoda et al., 2002). Because of these reasons, quantum efficiency is dramatically less than unity. That is, not all incident photons are absorbed to create electrical current. On the other hand, quantum efficiency doesn't contain photon energy, so responsivity is more commonly used for determining the characterization of the PIN photodiode. Responsivity is called as,

$$R = \frac{I_p}{P_0} \left(\frac{A}{W} \right) \quad (6)$$

Where I_p refers to photocurrent in watt and P_0 refers to optical power in watt. Responsivity can be fostered with quantum efficiency expression,

$$r_p = \frac{P_0}{hf} \quad (6.1)$$

we can obtain r_e easily with Eq. (5.1).

$$r_e = \eta r_p \quad (6.2)$$

$$r_e = \frac{\eta P_0}{hf} \quad (6.3)$$

The Output photocurrent is derivated simply from Eq.(6.3) by multiplying the charge of the electron

$$I_0 = \frac{\eta P_0 e}{hf} \quad (6.4)$$

From Eq. (6.4) we can easily find responsivity wavelength relation,

$$R = \frac{\eta e \lambda}{hc} \quad (6.5)$$

According to the derivated equation, the responsivity of the photodetector is directly proportional to quantum efficiency. Ideal quantum efficiency and responsivity are represented in Figure 3.12 (Senior and Jamro, 2009).

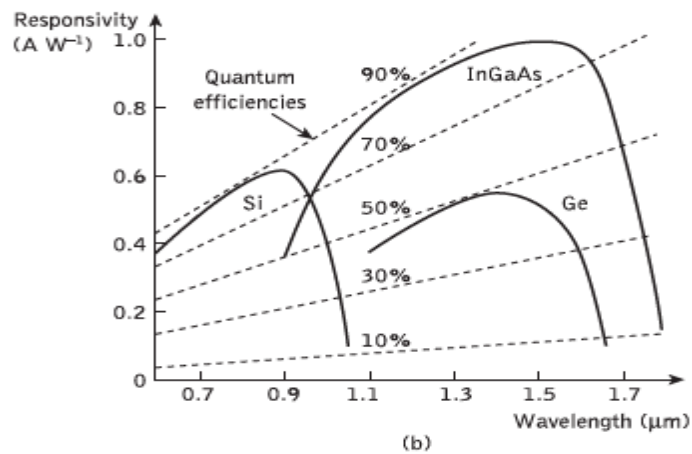
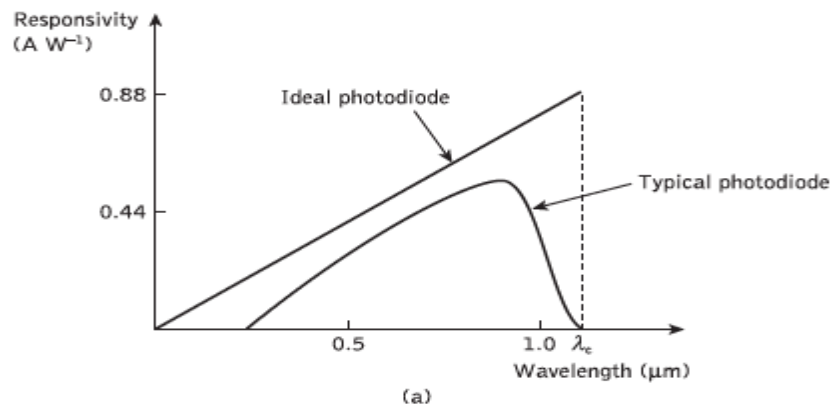


Figure 3.12. a) Ideal responsivity characteristic b) Quantum efficiency of materials (Senior and Jamro, 2009)

4. MATERIAL AND METHODS

4.1 Fabrication of Silicon PIN Photodiode

Silicon PIN photodiode fabrication process is classified into three main applications. These three processes are followed Radio Corporation of America (RCA) cleaning process, initial oxide process, and conventional photolithography application, respectively.

4.1.1 Cleaning Process of Silicon Wafer

There are some contaminants on the surface of the Silicon wafer. These contaminants have to be removed in order to get high performance from Silicon PIN diode. Therefore, we used the RCA procedure that is industry standard for removing the contaminant from the wafer. There are several steps for the RCA procedure. These are organic clean, oxide strip and ionic clean.

- a) **Organic clean:** Organic clean that removes organic contaminant with 20 L of deionized water, 2 L NH_4OH , and 2 L H_2O_2 . This solution ratio is equal to 10:1:1 (Distilled H_2O , H_2O_2 , NH_4OH), and the solution is heated to 60 °C. Wafers are put in this solution for 10 minutes and then they are taken with carries and put in distilled water for 4 cycles quick dump.
- b) **Oxide strip:** Thin SiO_2 layer may be grown on the wafer and some fraction of ionic contaminants likely to remain. In order to remove these unwanted contaminants, HF (Hydrofluoric acid) solution was prepared with distilled water H_2O . After that Silicon wafers are put into HF solution during ten seconds. They are removed from HF bath and we put them in distilled water for 4 quick dump cycles.
- c) **Ionic Cleaning:** Ionic cleaning removes the ionic contaminant, such as Na^+ Fe^+ with 20 L of deionized water, 2 L HCl and 2 L H_2O_2 in which we located our silicon wafer for ten minutes at 60 °C. After ten minutes silicon wafers are put into deionized water for 7 cycles quick dump.

4.1.2 Initial Field Oxide Deposition

Silicon dioxide layer has the vital role to prevent slickness of silicon wafer during the photolithography process. So, 793-nm field oxide (SiO_2) area, which is shown in Figure 4.1, was grown on cleaned 6 inch (100) 500- μm thick slightly doped 2.4 k Ω -2.8 k Ω N-type Silicon wafer with wet oxidation procedure at a high temperature (1100 °C) in a diffusion oven (Figure 4.2).

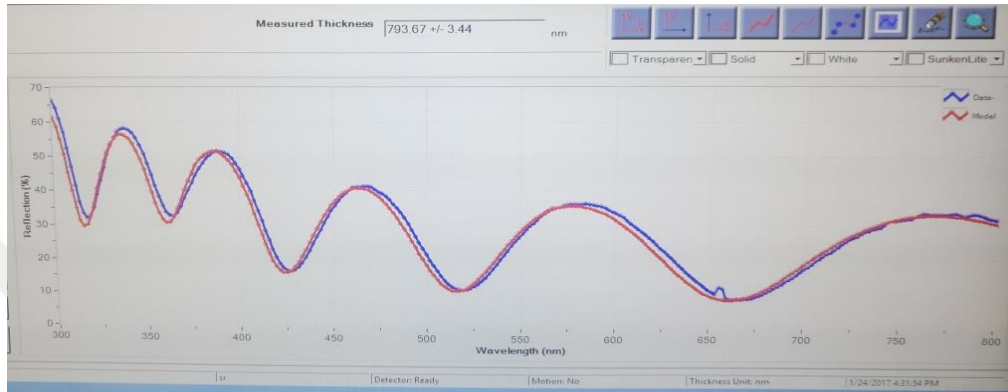


Figure 4.1. Spectroscopy measurement of a silicon wafer



Figure 4.2. Silicon Oxide on a silicon wafer

4.1.3 Photolithography Process for Phosphorus Deposition

A photolithography process is utilized to transfer the pattern onto a Silicon wafer by the photomask. For this application, the following steps were applied. Firstly, Silicon wafers were covered with photoresist by using spin coater at 7500 rpm during 15-second (Figure 4.3).

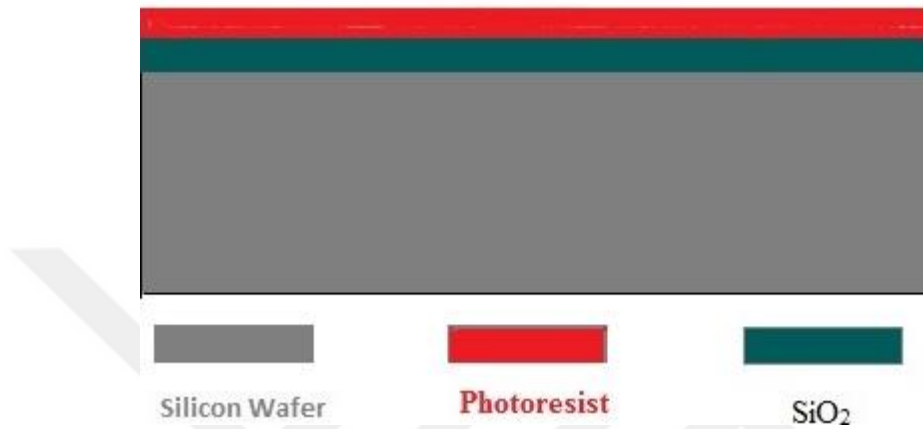


Figure 4.3. The photoresist on a silicon wafer

Then, this application enables us to create a canal to deposit phosphorus with ultraviolet exposure shown in Figure 4.4.

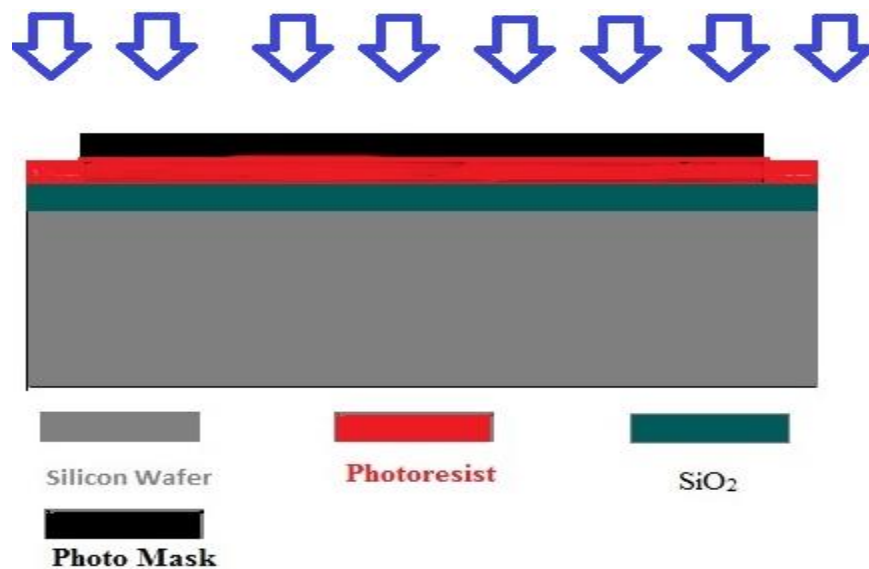


Figure 4.4. Ultraviolet exposure on a silicon wafer

The photoresist on the Silicon wafer was spoiled under the ultraviolet array. Then Silicon wafers were sunk into developer solution to remove spoiled photoresist. Having been sunk into the developer, Silicon wafers were put in BHF solution for wet etching to remove SiO₂ layer (Figure 4.5).

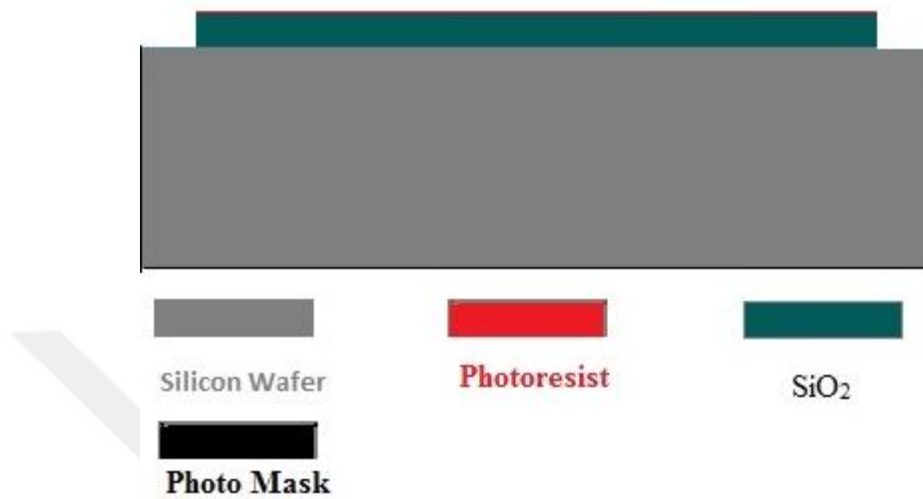


Figure 4.5. Silicon wafer representation after initial lithography

Silicon wafers are shown in Figure 4.5 has a resistivity of 2.4 -2.8 k Ω which is measured using the four-point method. Next, the N-type region was constructed with thermal phosphorus deposition, and we obtained a 0.55 Ω cm wafer. After that, wafers were put in diffusion oven for drive-in with which we were able to expand N-type and grow by 120 nm thick SiO₂ layer via dry oxidation methods at 950 °C. The measured resistivity of Si surface is 0.27 Ω cm after drive-in process These processes are shown in Figure 4.6(a) and Figure 4.6(b).

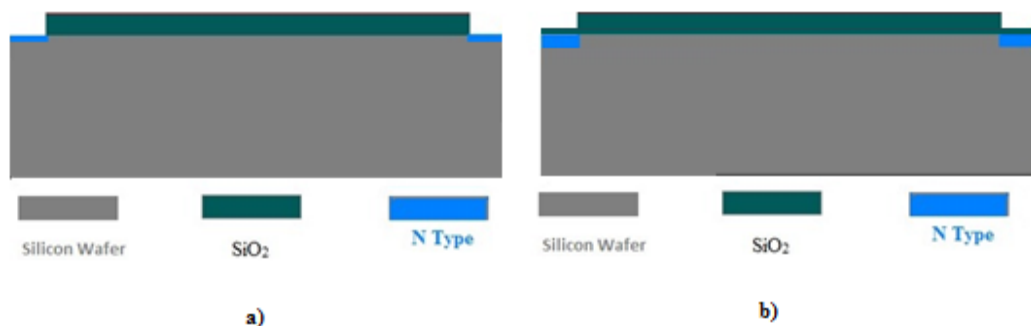


Figure 4.6. a) Wafer structure after phosphorus deposition process b) Wafer structure after drive-in the process

4.1.4 Photolithography Process for Boron Deposition

Another photolithography process was applied on a Silicon wafer that is shown in Figure 4.7. These wafers were covered again with photoresist, and the ultraviolet array was exposed on them to spoil photoresist. Afterward, the spoiled photoresist is removed with a developer solution and hard baked. Then wafers were put in BHF solution which was prepared with 235 gr NF_4 , 370 ml of deionized water and 120 ml HF solution. For 8 min, BHF solution was removing the SiO_2 layer. Finally, we put wafers in a stripper to remove the remaining photoresist, and this process is shown in Figure 4.7.

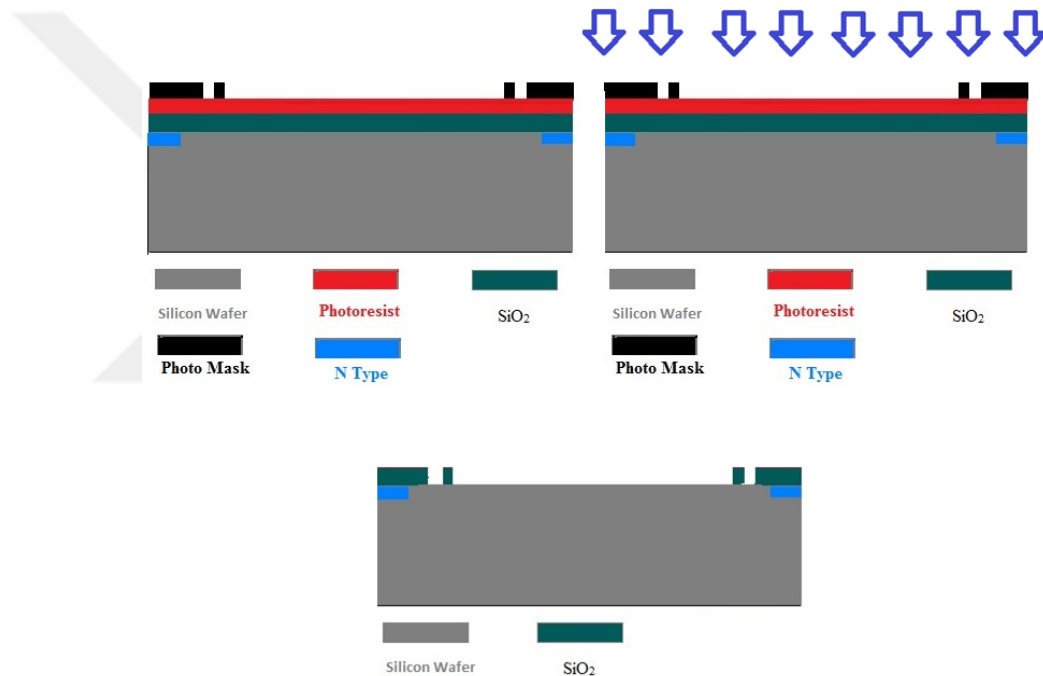


Figure 4.7. Photolithography process for boron deposition

Next, 100 nm P-type region was constructed by Boron deposition at thermal diffusion oven in Figure 4.8(a). Then these wafers, which have 3.8 Ωcm resistivity, are located in diffusion oven again for a drive-in process at 950 °C to create small silicon dioxide layer. After a drive-in, we obtained 4.7 Ωcm resistivity structure and P⁺ region expanded to 120nm shown in Figure 4.8(b).

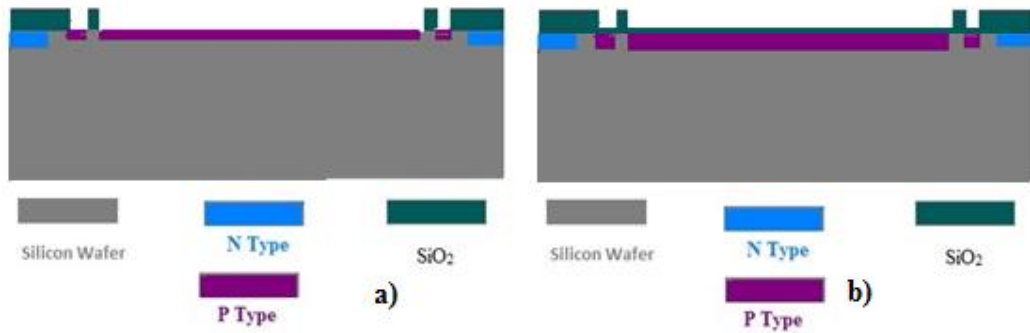


Figure 4.8. a) Wafer structure after boron deposition b) Wafer structure after drive-in the process

4.1.5 Photolithography Process for Metallization

Photoresists and photomask were covered onto wafers to open a channel for aluminum deposition. Afterwards, ultraviolet was exposed on the wafer to spoil photoresist in Figure 4.9.

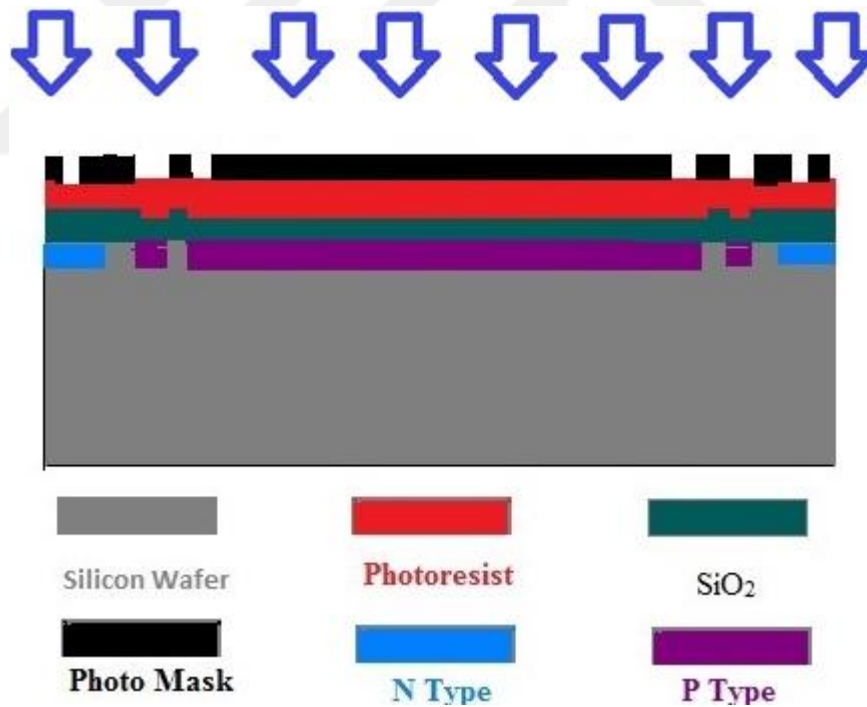


Figure 4.9. Ultraviolet light exposure

Then same photolithography process was applied to remove spoiled photoresist and SiO₂ layer as shown in Figure 4.10.



Figure 4.10. Wafer structure after liftoff process

Then wafers were covered with Aluminum (Al) by sputtering at 175 W for 15min. Afterwards, they were covered with photoresist and photomask for the removing process. Then they were exposed to the ultraviolet array as shown in Figure 4.11.

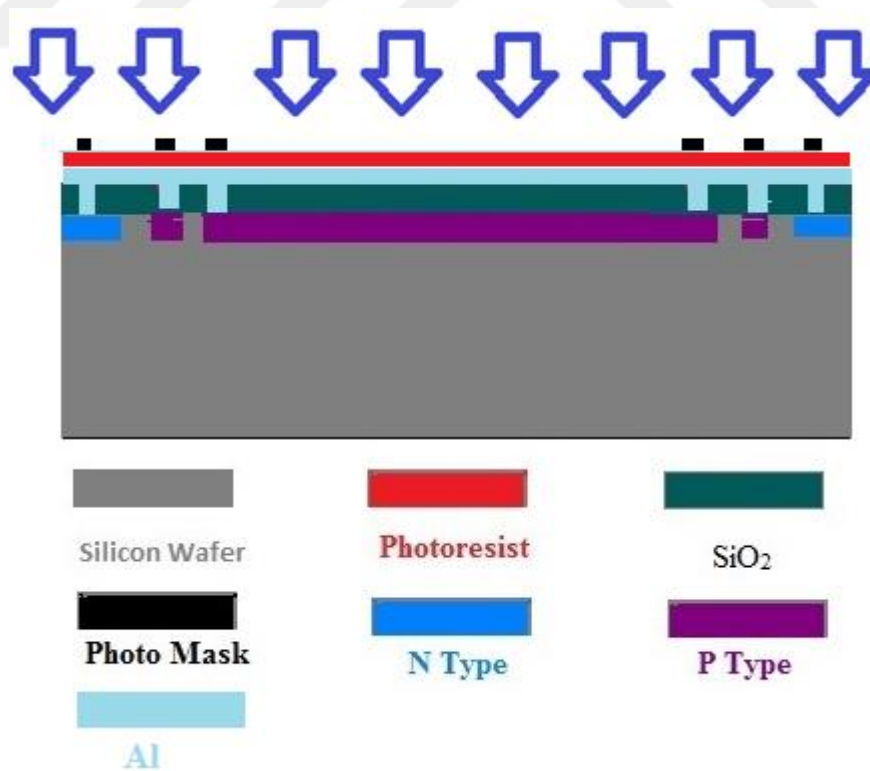


Figure 4.11. Ultraviolet exposure on a silicon wafer to spoil photoresist

After that, Aluminum was removed with a solution that contains H_3PO_4 , HNO_3 , CH_3COOH , and PIN photodiode structure was obtained as shown in Figure 4.12.

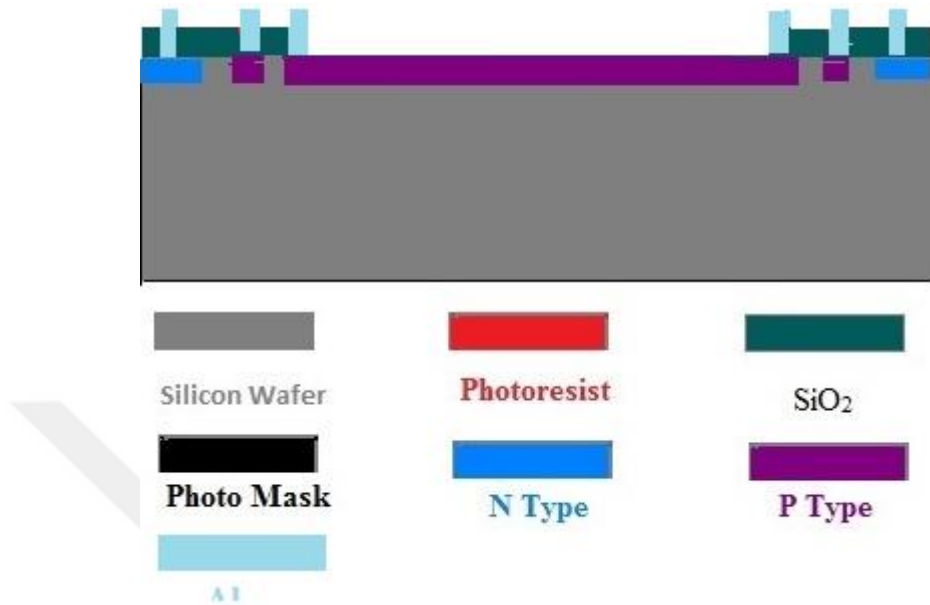


Figure 4.12. Schematic representations of PIN photodiode structure

After Fabrication steps, Silicon wafers were cut by dicing machine precisely. Then, Separated PIN photodiodes were bonded to plastic package apparatus by wire-bonding machine. Last PIN photodiodes' structure is represented in Figure 4.13

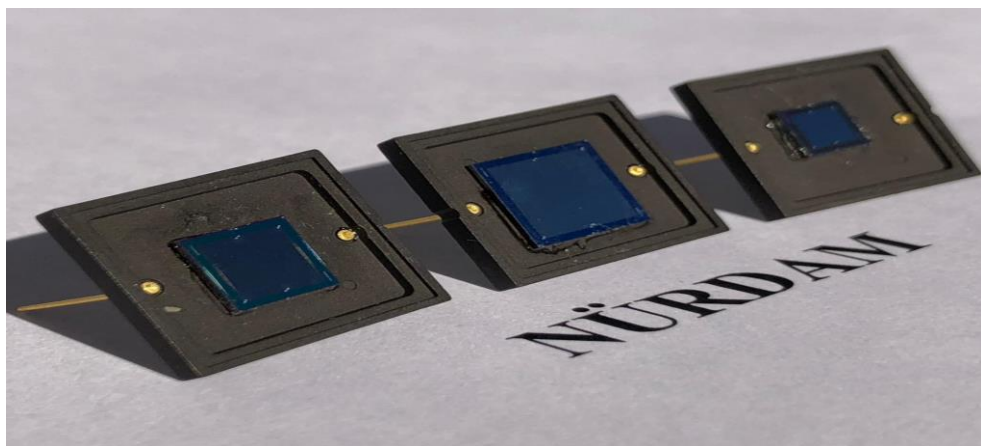


Figure 4.13. Fabricated PIN photodiode structure

4.2 Device Characteristic of Silicon PIN Photo Diode

4.2.1 Current-Voltage Characteristic Measurement

Current-Voltage (I-V) characteristic is one of the most crucial electrical feature which was determined by KEITHLEY 2636B SYSTEM source meter and I-V characteristic computer measurement software. The I-V measurement software was adjusted to sweep from 5 to -120 V. Current values were observed at the computer software under dark conditions at room temperature.

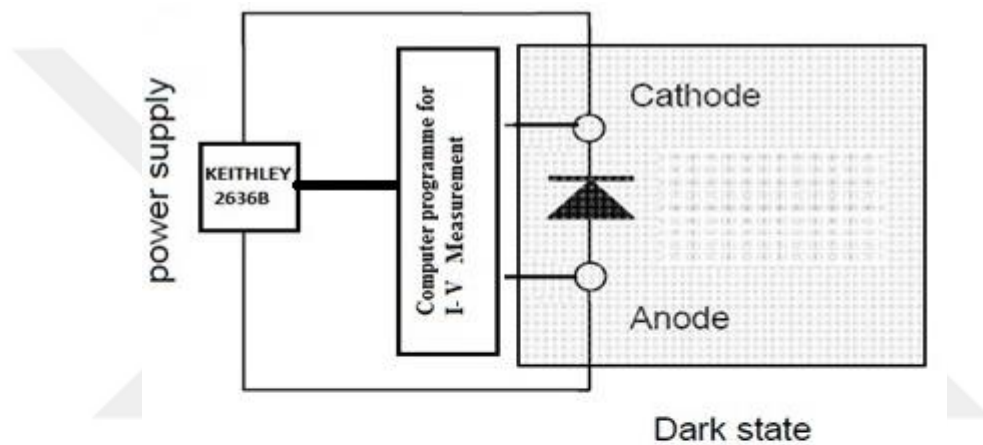


Figure 4.14. I-V measurement system

4.2.2 Capacitance-Voltage Characteristic Measurement

The capacitance of Silicon PIN photodiode was measured with HIOKI 3532-50 LCR Hitester and KIKUSUI bipolar power supply PBZ40-10. Voltage swept from 5 Volt to -30 Volt at 1MHz. Then capacitance values were obtained respectively for each voltage steps at Lab-view software.

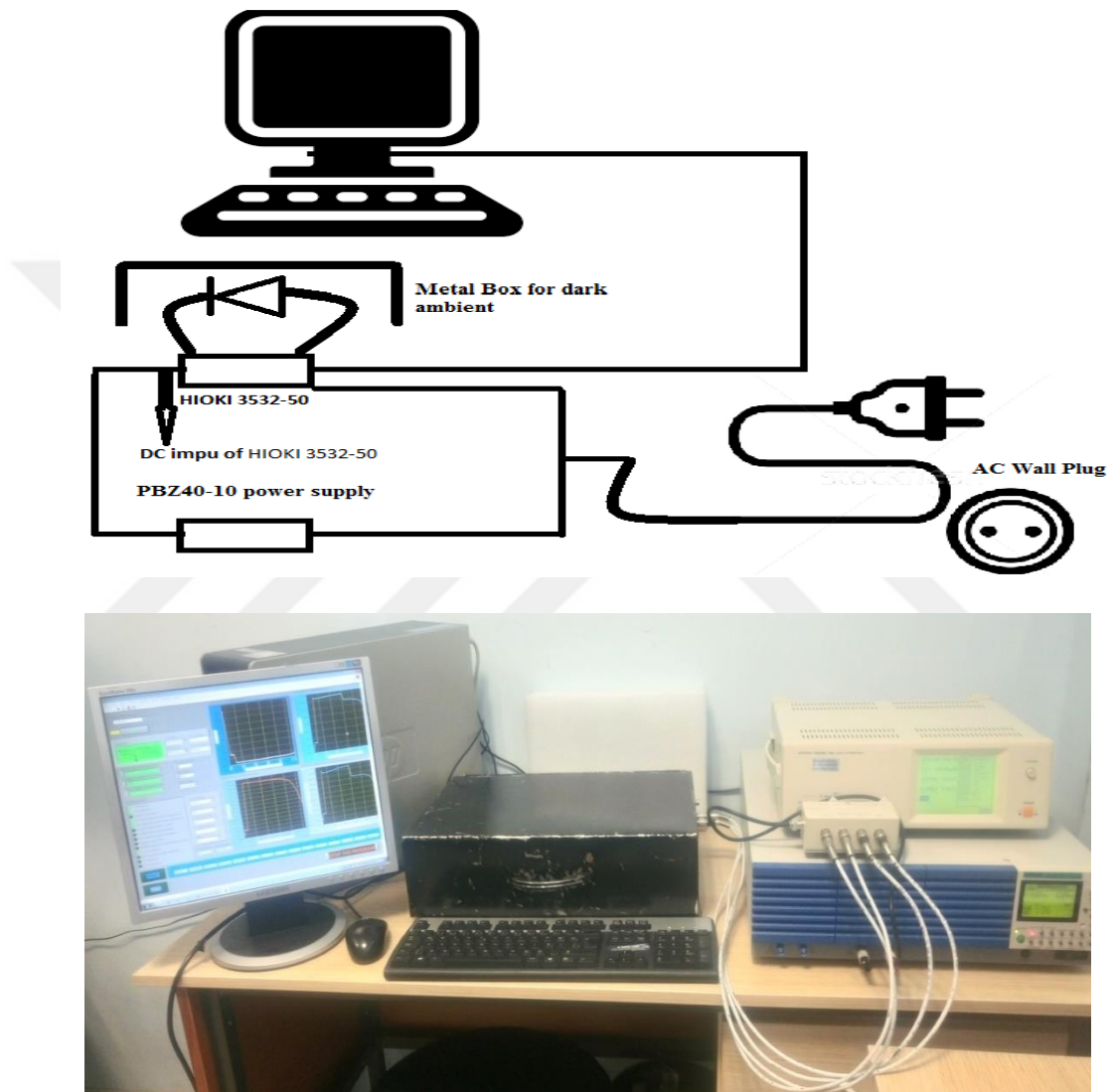


Figure 4.15. C-V measurement system

4.2.3 Quantum Efficiency and Spectral Response Measurement

Quantum efficiency and spectral responsivity measurements were carried out to determine the spectral range and the quantum efficiency under the various light spectrum of Silicon-based PIN photodiode by using PVE 300 Photovoltaic EQE (IPCE) and IQE solution at METU-GUNAM. The measurement system in Figure 4.16 which has 75W Xenon and 100W Quartz Halogen light source, was adjusted 10 nm wavelength, sweeping between 300 nm and 1150 nm. Then, the calibration settings were done by taking account of the active area of each PIN photodiode to fall into light beam, precisely upon the active area, and prevent undesirable optical losses during measurement.



Figure 4.16. Spectral responsivity and quantum efficiency measurement system

5. EXPERIMENTAL RESULTS AND DISCUSSIONS

5.1 Measurement Results of Fabricated Silicon PIN Photodiode

5.1.1 Results of Capacitance -Voltage Characteristic

Capacitance-Voltage measurement was carried out for Silicon-based PIN photodiodes that have $3.5 \times 3.5 \text{ mm}^2$, $5.0 \times 5.0 \text{ mm}^2$, $7.0 \times 7.0 \text{ mm}^2$ active area to investigate depletion region capacitance on conductive mode (reverse biased). According to our results that are shown in Figure 5.1. Capacitance values for each Silicon PIN photodiode were dropped exponentially until -5V (fully depleted voltage). After PIN diodes reached to the depletion voltage, capacitance values decreased slightly. The observed small capacitance changes are related to the unwanted parasitic capacitance which is ignored in the photodetector application. This capacitance behavior can be explained by electrostatic potential which is created with reverse biased, and with the risen total junction potential, it expands depletion region that reduces capacitance (Sze, 1985). Having been fabricated, Silicon PIN photodiodes reach to fully depleted mode, at which capacitances values of $3.5 \times 3.5 \text{ mm}^2$, $5.0 \times 5.0 \text{ mm}^2$, $7.0 \times 7.0 \text{ mm}^2$ PIN photodiodes are 23 pf, 41 pf, 61 pf respectively. Obtained results showed that the junction capacitance of Silicon PIN photodiode is inversely proportional to reverse biased and directly proportional to active of PIN photodiode. This correlation is simply explained with Eq (4.4). Our experimental results are consistent with studies that have already published (Kim et al., 2014; Seto et al., 1997) Secondly, impurity concentration was calculated from slope of $C^{-2}(F^{-2})$ -voltage (V) graph (Suzuki et al., 2013) and the results for Figure (5a), (5b), and (5c) are $3.45 \times 10^{12} \text{ cm}^{-3}$, $2.42 \times 10^{12} \text{ cm}^{-3}$, $1.78 \times 10^{12} \text{ cm}^{-3}$ respectively.

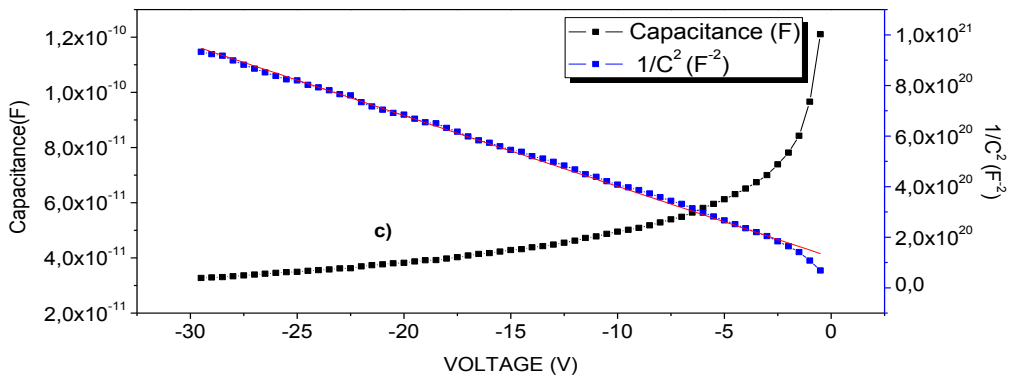
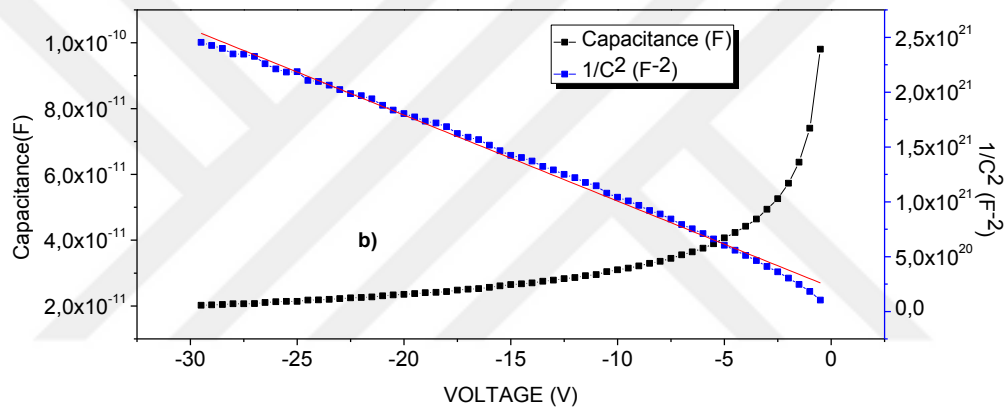
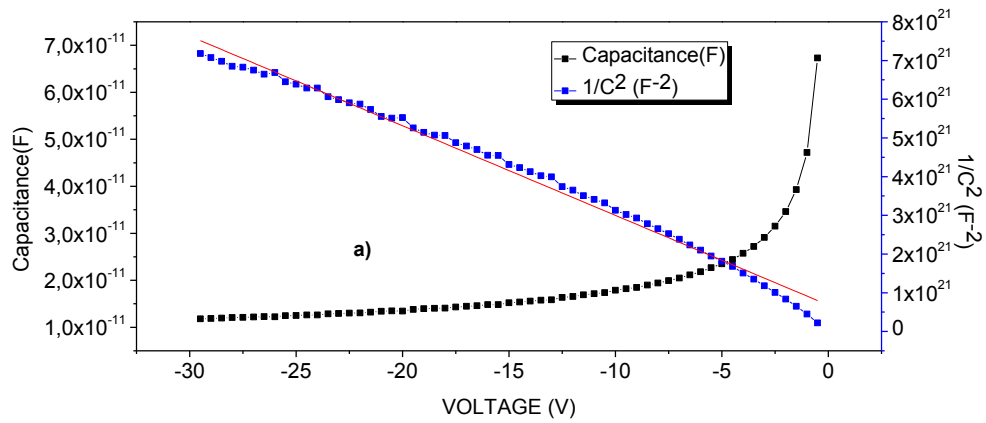


Figure 5.1. a) Reverse biased C-V and C^{-2} -V characteristics $3.5 \times 3.5 \text{ mm}^2$ PIN diode b) Reverse biased C-V and C^{-2} -V characteristics $5.0 \times 5.0 \text{ mm}^2$ PIN diode c) Reverse biased C-V and C^{-2} -V characteristics $7.0 \times 7.0 \text{ mm}^2$ PIN diode

5.1.2 Results of Current-Voltage Characteristic

Current-Voltage (I-V) characteristic was studied on reversed biased for Silicon PIN photodiodes which have different active areas. As expected, break down phenomena was observed at high reverse voltage. This phenomenon generally observed because of the band to band tunneling (Sze, 2007). The break down voltages for 7.0 x 7.0 mm², 5.0 x 5.0 mm² and 3.5 x 3.5 mm² PIN photodiodes are -93 V, -84 V and -77.5V respectively. Dark current, namely leakage currents, at the breakdown voltage are -10.8 μA, -10 μA, -10.2μA in Figure 5.2(a). These obtained results were also given in Table 1. Even if these obtained current values are so high according to reported studies (Cho et al., 2006; Kim et al., 2015), fabricated PIN photodiodes have leakage current order of 10 nA between -5V and -23V. Observed leakage currents at low voltage can be explained with Silicon temperature dependence (Ahmed, 2007). On the other hand, leakage current at high voltage can be related to tunneling current instead of temperature dependence (Feng et al., 2018; Suzuki et al., 2013). We also calculated dark current density simply by using dark current data function of voltage in Figure 5.2 (b). Reverse dark current density dropped linearly with active area increase between 5x5mm² and 7.0 x 7.0mm² from 65x10⁻⁹ A/cm² to -39 x10⁻⁹ A/cm² but 5.0x5.0mm² PIN photodiode has higher current density than 3.5x3.5mm² PIN photodiode, whose values 57x10⁻⁹ A/cm² due to surface recombination of PIN photodiodes. Leakage current that results from temperature dependence and surface recombination-generation can be eliminated by passivation methods (Kemmer, 1984; Resnik et al., 2000).

Table 1. Some electrical parameters of fabricated PIN photodiodes

Active Area (mm ²)	Dark Current @ -5V (nA)	Break Down Voltage at 10 μA (-V)	Capacitance @ -5V (pF)	Doping Concentration (x10 ¹² cm ⁻³)
7.0 x 7.0	-19.1	93	61	1.78
5.0 x 5.0	-16.5	84	41	2.42
3.5 x 3.5	-6.97	77.5	23	3.45

In addition, shunt resistances were calculated experimentally from current values for PIN photodetector by applying small reverse voltage on PIN photodiodes. Resistance values for $7.0 \times 7.0 \text{ mm}^2$, $5.0 \times 5.0 \text{ mm}^2$, $3.5 \times 3.5 \text{ mm}^2$ diodes. $50 \text{ M}\Omega$, $75 \text{ M}\Omega$, and $155 \text{ M}\Omega$ respectively.

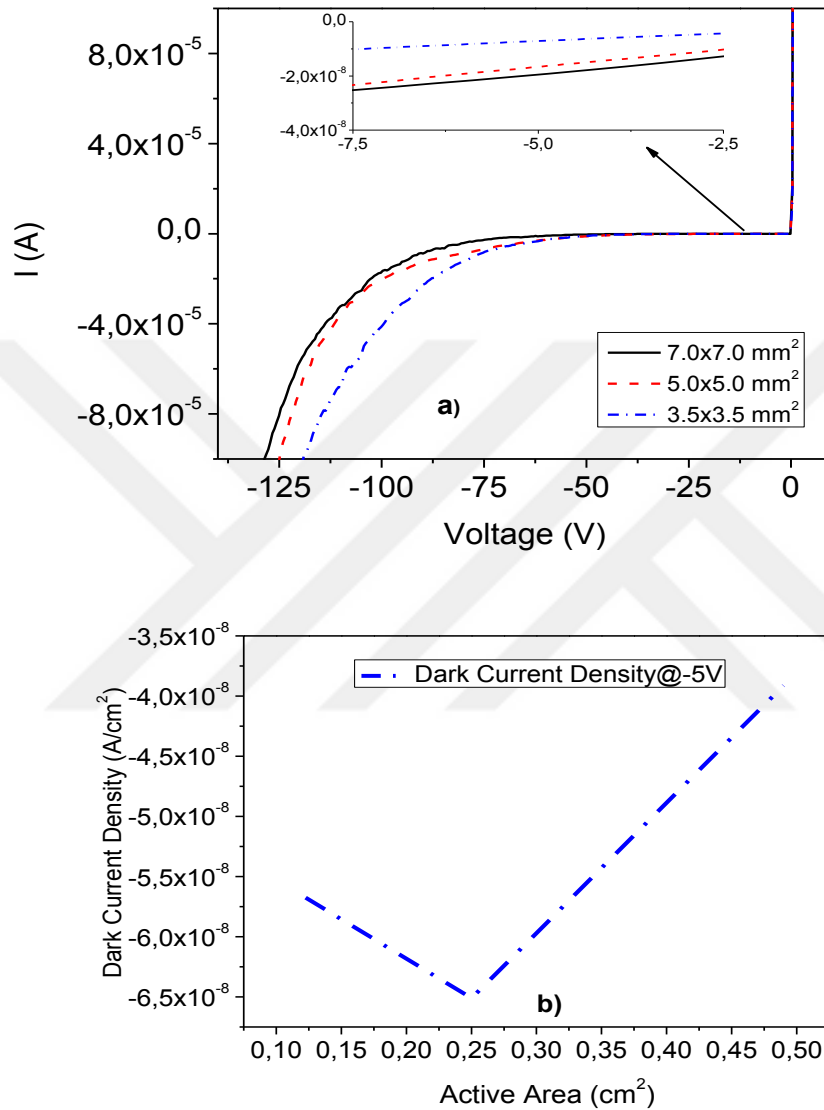


Figure 5.2. a) Reverse biased dark current measurement at 295K **b)** Reverse dark current density function of the PIN photodiode active area at -5 V

5.1.3 Results of Quantum Efficiency and Spectral Response

Quantum efficiency and spectral responsive measurements were done for PIN photodiodes which have a different active area at zero biased and at room temperature. For this purpose, the light source between 300 nm and 1150 nm, precisely aligned on the active area of PIN diodes. During the measurement the first detection was observed at 380 nm. This means that smaller wavelengths below 380 nm electron-hole pairs come up closer to the surface, in where recombination time is so short. Thus, they cannot be collected by a PIN photodiode. This situation indicates a short cut off wavelength is 380 nm for our PIN photodiodes. After 380nm wavelength, quantum efficiency and responsivity values increased rapidly until peak wavelength and then dropped till 1100 nm which is long cut off wavelength in Figure 5.3. After the long cut off wavelength, the incident wave doesn't have sufficient energy to excite an electron from the valence band to conduction band. That is, long cut off wavelength depends on the temperature on account of the energy level of the band gap of material, and the low cut off wavelength is related to material coefficient (Yotter and Wilson, 2003).

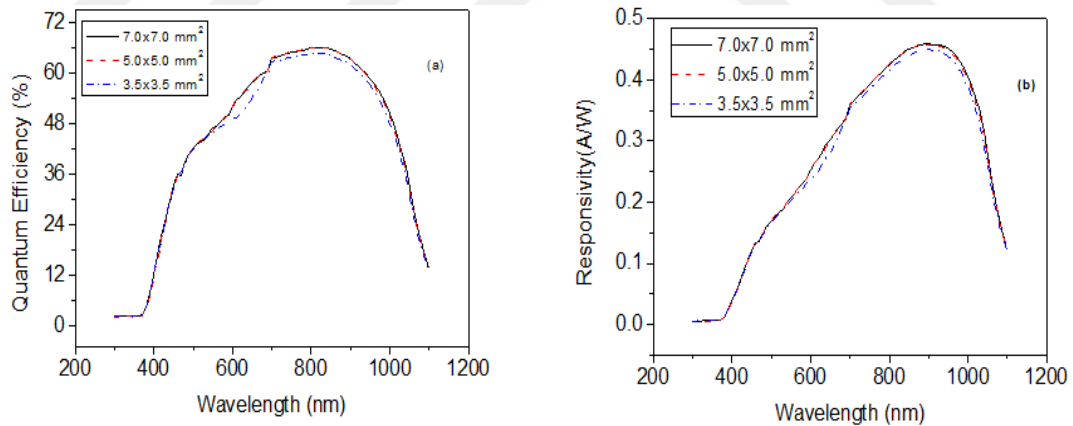


Figure 5.3.a) Quantum efficiency measurement characteristic b) Spectral responsivity measurement characteristic

Obtained results for all Silicon PIN photodiodes are consistent with Silicon PIN photodiode characteristic (Boivin, 2001; Sze, 1985; Yotter and Wilson, 2003). However, responsivity values are worse than commercial Silicon PIN photodiodes, such as Hamamatsu S5870, S5980. But the obtained results can be improved by covering anti-reflect layer to prevent unwanted reflection.

As shown in Table 2, the quantum efficiency and spectral response values are the same for 7.0x7.0 mm² and 5.0x5.0mm² Silicon PIN photodiode but, for 3.5x3.5 mm² small amount of optical loose was observed. This situation results from spot-size active area uniformity

Table 2. Quantum efficiency and Spectral response results

Active Area	3.5x3.5 mm ²	5.0x5.0 mm ²	7.0x7.0 mm ²
Short Cutoff Wavelength (nm)	380	380	380
Peak Wavelength λ_p (nm)	820	820	820
Long Cutoff Wavelength (nm)	1100	1100	1100
Quantum Efficiency(%) λ_p	64.70	66.06	66.05
Responsivity (AW ⁻¹) λ_p	0.43	0.44	0.44

6. CONCLUSION AND RECOMMENDATION

During this study, planar Silicon-based PIN photodiodes with different active areas have been fabricated on the (100) intrinsic silicon wafers by using a conventional photolithography process. In order to create n and p regions, thermal phosphorous diffusion (using POCl_3) and thermal boron diffusion (using BBr_3) were used at 950°C in clean room environment at Bolu Abant İzzet Baysal University Center of Nuclear Radiation Detector Research and Application Center.

Having been fabricated, $7.0 \times 7.0 \text{ mm}^2$, $5.0 \times 5.0 \text{ mm}^2$, $3.5 \times 3.5 \text{ mm}^2$ Silicon-based PIN photodiodes of the current-voltage analysis indicated that break down phenomena is observed at high reverse voltage, at which leakage currents values are the order of μA but the order of nA between -5V and -10V . These results are high because of material temperature dependence, and tunneling current which is observed at high reversed biased voltage. In addition, current densities of diodes were calculated from dark current values function of area and current density between $5.0 \times 5.0 \text{ mm}^2$ PIN diode and $7.0 \times 7.0 \text{ mm}^2$ PIN diode decreased linearly while active area rose, but the current density of $3.5 \times 3.5 \text{ mm}^2$ Silicon PIN diode is less than $5.0 \times 5.0 \text{ mm}^2$. This situation showed that surface recombination on depletion can be observed for $5.0 \times 5.0 \text{ mm}^2$ PIN photodiodes. Shunt resistances of diodes were found at $50 \text{ M}\Omega$, $75 \text{ M}\Omega$, and $155 \text{ M}\Omega$ respectively. Another crucial parameter is that capacitances have evaluated the function of voltage for all Silicon PIN photodiode. Junction capacitance decreased exponentially with applied reverse biased to the order of pF till -5 V (fully depleted voltage). Then small capacitance decline was observed at higher reverse-biased voltage. This observed capacitance is related to parasitic capacitance. Ion concentration (n_i) was calculated from $1/C^2$ slope. The results are $1.78 \times 10^{12} \text{ cm}^{-3}$, $2.42 \times 10^{12} \text{ cm}^{-3}$, $3.45 \times 10^{12} \text{ cm}^{-3}$. In order to determine the optical feature of Silicon PIN photodiodes, quantum efficiency and responsivity measurements were done. Quantum efficiency and responsivity possess same value for $7.0 \times 7.0 \text{ mm}^2$ and $5.0 \times 5.0 \text{ mm}^2$ PIN photodiodes. This is an expected result for Silicon PIN photodiodes, but small optical loss was observed for $3.5 \times 3.5 \text{ mm}^2$ photodiode owing to spot-size is not precisely fit with active area of Silicon

PIN photodiode. Silicon PIN diodes can detect wavelengths between 380nm and 1100nm. The maximum efficiency was obtained at 810 nm. This result is consistent with the theoretical result of Silicon PIN photodiodes.

Consequently, Silicon-based PIN photodiodes were fabricated successfully, and electrical and optical measurements were carried out. According to the obtained results, fabricated PIN photodiodes can be operated between -5 voltage and breakdown voltage. In addition, PIN photodiodes sensitive light spectrum between 380 nm and 1100 nm. Even if the leakage current is the main problem for our PIN photodiodes, it can be eliminated with some structural optimization for future work. In addition, this study was a big step to fabricate radiation detector, vivo dosimeter and so on, using Silicon PIN photodiode. The fabricated PIN diodes can be used in optoelectronic applications

7. REFERENCES

- Ahmed SN (2007) *Physics and Engineering of Radiation Detection*, First ed, Elsevier 2007, London, UK.
- Barthe J (2001) "Electronic dosimeters based on solid state detectors", *Nuclear Instruments & Methods in Physics Research Section B-Beam Interactions with Materials and Atoms*, 184 (1-2): 158-189.
- Ben S, Sanjay B (2005) *Solid State Electronic Devices* 6th ed, Prentice Hall, 2005.
- Boivin LP (2001) "Spectral responsivity of various types of silicon photodiode at oblique incidence: comparison of measured and calculated values", *APPLIED OPTICS*, 40 (4): 485-491.
- Bowers JE, Burrus CA (1987) "Ultrawide-Band Long-Wavelength P-I-N Photodetectors", *Journal of Lightwave Technology*, 5 (10): 1339-1350.
- Boylestad RL (2013) *Electronic Devices and Circuit Theory*, 11 ed, Pearson Education, Inc., United States of America.
- Cho NI, Nam HG, Cha KH, Lee KH, Noh SJ (2006) "Fabrication of silicon PIN diode as proton energy detector", *Current Applied Physics*, 6 (2): 239-242.
- Feng YJ, Li C, Liu QL, Wang HQ, Hu AQ, He XY, Guo X (2018) "Scalability of dark current in silicon PIN photodiode", *Chinese Physics B*, 27 (4): 048501-048501
- Goushcha AO, Metzler RA, Hicks C, Kharkyanen VN, Berezetska NM (2004) "Determination of the carrier collection efficiency function of Si photodiode using spectral sensitivity measurements", *Semiconductor Photodetectors*, 5353: 12-19.
- Gray B, 2006. *Photo Diodes*, Wiley Encyclopedia of Biomedical Engineering John Wiley & Son, Inc.
- Kemmer J (1984) "Improvement of Detector Fabrication by the Planar Process", *Nuclear Instruments & Methods in Physics Research Section a Accelerators Spectrometers Detectors and Associated Equipment*, 226 (1): 89-93.
- Kim HS, Jeong M, Kim YS, Ha JH, Cho SY (2014) "Effect of temperature on silicon PIN photodiode radiation detectors", *Journal of the Korean Physical Society*, 64 (5): 651-654.

- Kim HS, Jeong M, Kim YS, Lee DH, Cho SY, Ha JH (2015) "Characteristics of fabricated si PIN-type radiation detectors on cooling temperature", Nuclear Instruments & Methods in Physics Research Section a-Accelerators Spectrometers Detectors and Associated Equipment, 784: 131-134.
- Kittel C (2005) Introduction to Solid State Physics, Eight ed, John Wiley & Sons, Inc, Newyork.
- Kumar R, Sharma SD, Philomina A, Topkar A (2014) "Dosimetric Characteristics of a PIN Diode for Radiotherapy Application", Technology in Cancer Research & Treatment, 13 (4): 361-367.
- Kyomasu M (1995) "Development of an Integrated High-Speed Silicon Pin Photodiode Sensor", Ieee Transactions on Electron Devices, 42 (6):1093-1099.
- Luryi S, Kastalsky A, Bean JC (1984) "New Infrared Detector on a Silicon Chip", Ieee Transactions on Electron Devices, 31 (9): 1135-1139.
- Ma S, Li Y, Zhang L, Wang J, Jin Y (2010) "Design and fabrication of large ultra-thin PIN detector with membrane stress deviation", Journal of Instrumentation, 5.
- Menon PS, Visvanathan NV, Shaari S (2004) "Development of silicon planar P-I-N photodiode", Penerbit Universiti Sains Malaysia, 20-21 December 2004, Universiti Sains Malaysia, Pulau Pinang.
- Mishra V, Srivastava VD, Kataria SK (2005) "Role of guard rings in improving the performance of silicon detectors", Pramana-Journal of Physics, 65 (2):259-272.
- Nicollian EH, Brews JR (2003) Silicon Surface, Mos(Metal Oxide Semi Conductor) Physics and Technology. A John Wiley & Sons, Inc, Publication Canada
- Onoda S, Hirao T, Laird JS, Mori H, Okamoto T, Koizumi Y, Itoh H (2002) "Spectral response of a gamma and electron irradiated pin photodiode", Ieee Transactions on Nuclear Science, 49 (3): 1446-1449.
- Razavi B (2015) Microelectronics, Second ed, John Wiley & Sons (Asia)Pre Ltd USA.
- Resnik D, Krizaj D, Vrtacnik D, Amon S, 2000. Process considerations in reducing leakage current of PIN radiation detectors, Proceedings of the 2000 Third IEEE International Caracas Conference on Devices, Circuits and Systems. IEEE.
- Rieke GH (2002) Detection of Light, Detection of Light. Cambridge University Press, United States of America, New York

- Senior JM, Jamro MY (2009) *Optical Fiber Communications: Principles and Practice*, Third ed, Financial Times/Prentice Hall.
- Seto M, Mabesoone M, DeJager S, Vermeulen A, DeBoer W, Theunissen M, Tuinhout H (1997) "Performance dependence of large-area silicon p-i-n photodetectors upon epitaxial thickness", *Solid-State Electronics*, 41(8):1083-1087.
- Simon A, Kalinka G (2005) "Investigation of charge collection in a silicon PIN photodiode", *Nuclear Instruments & Methods in Physics Research Section B-Beam Interactions with Materials and Atoms*, 231: 507-512.
- Suzuki M, Sakai T, Makino T, Kato H, Takeuchi D, Ogura M, Okushi H, Yamasaki S (2013) "Electrical characterization of diamond PIN diodes for high voltage applications", *Physica Status Solidi a-Applications and Materials Science*, 210 (10): 2035-2039.
- Sze SM (1985) *Semiconductor Devices*, First ed, United State Of America.
- Sze SM (2002) *Semiconductor Devices Physics and Technology*, Second ed, JOHN WILEY & SONS, INC., United State.
- Sze SM (2007) *Physics of Semiconductor Devices*, Third ed, John Wiley & Sons, Inc., Canada.
- Tucker RS, Taylor AJ, Burrus CA, Eisenstein G, Wiesenfeld JM (1986) "Coaxially Mounted 67 Ghz Bandwidth Ingaas Pin Photodiode", *Electronics Letters*, 22 (17): 917-918.
- Von Ammon W, Herzer H (1984) "The Production and Availability of High-Resistivity Silicon for Detector Application", *Nuclear Instruments & Methods in Physics Research Section a-Accelerators Spectrometers Detectors and Associated Equipment*, 226 (1): 94-102.
- Wood TH, Burrus CA (1984) "Highspeed optical modulation with GaAs/GaAlAs quantum wells in a pin diode structure", *Applied Physics Letters*, 44 (16): 16-18.
- Xu Y (2015) *Fabrication And Characterization Of Photodiodes For Silicon Nanowire Applications And Backside Illumination*, Master Degree, University of Dayton the School of Engineering, Dayton, Ohio.
- Yamamoto K, Fujii Y, Kotooka Y, Katayama T (1987) "Highly Stable Silicon Pin Photodiode", *Nuclear Instruments & Methods in Physics Research Section a-Accelerators Spectrometers Detectors and Associated Equipment*, 253 (3): 542-547.
- Yamamoto M, Kubo M, Nakao K (1995) "Si-OEIC with a Built-in Pin-Photodiode", *Ieee Transactions on Electron Devices*, 42 (1): 58-63.

Yotter RA, Wilson DM (2003) "A review of photodetectors for sensing light-emitting reporters in biological systems", IEEE SENSORS JOURNAL, 3 (3): 288-303.

Zhou CZ, Warburton WK (1996) "Comparison of silicon pin diode detector fabrication processes using ion implantation and thermal doping", Nuclear Instruments & Methods in Physics Research Section a Accelerators Spectrometers Detectors and Associated Equipment, 378 (3):529-530.



8. CURRICULUM VITAE

Name SURNAME : Emre DOĞANCI

Place and Date of Birth : BOLU 07.03.1990

Bachelor's Degree : Bolu Abant İzzet Baysal University

Master Degree : Bolu Abant İzzet Baysal University

E-mail : emredoganci8@gmail.com

Address : NRDC (BAIBU) BOLU/TURKEY